ISSN 2188-286X

マス・フォア・インダストリ研究 No.21

Fiber Topology Meets Applications

Organizer:

Daisuke Sakurai
Shigeo Takahashi
Naoki Hamada
Osamu Saeki
Hamish Carr
Takahiro Yamamoto

Institute of Mathematics for Industry
Kyushu University

About the Mathematics for Industry Research

The Mathematics for Industry Research was founded on the occasion of the certification of the Institute of Mathematics for Industry (IMI), established in April 2011, as a MEXT Joint Usage/Research Center – the Joint Research Center for Advanced and Fundamental Mathematics for Industry – by the Ministry of Education, Culture, Sports, Science and Technology (MEXT) in April 2013. This series publishes mainly proceedings of workshops and conferences on Mathematics for Industry (MfI). Each volume includes surveys and reviews of MfI from new viewpoints as well as up-to-date research studies to support the development of MfI.

October 2018
Osamu Saeki
Director
Institute of Mathematics for Industry

Fiber Topology Meets Applications

Mathematics for Industry Research No.21, Institute of Mathematics for Industry, Kyushu University
ISSN 2188-286X
Editors: Daisuke Sakurai, Shigeo Takahashi, Naoki Hamada, Osamu Saeki, Hamish Carr, Takahiro Yamamoto
Date of issue: 10 March 2021
Publisher:
Institute of Mathematics for Industry, Kyushu University
Motooka 744, Nishi-ku, Fukuoka, 819-0395, JAPAN
Tel +81-(0)92-802-4402, Fax +81-(0)92-802-4405
URL https://www.imi.kyushu-u.ac.jp/
Printed by
Kijima Printing, Inc.
Shirogane 2-9-6, Chuo-ku, Fukuoka, 810-0012, Japan
TEL +81-(0)92-531-7102 FAX +81-(0)92-524-4411

Fiber Topology Meets Applications

Organizer: Daisuke Sakurai
Shigeo Takahashi
Naoki Hamada
Osamu Saeki
Hamish Carr
Takahiro Yamamoto

Preface

In differential topology, the study of the topology of fibers, known as fiber topology, extends the Morse theory, of functions, to that of maps. This establishes a thorough exploration of topological transitions of inverse images. It has been proven powerful for understanding today's data whose size and complexity are overwhelming.

In recent years, fiber topology has been actively pushed forward from mathematical studies towards computation. While the computational approach for the Morse-case was studied separately, the two research domains started communication after some years. For more general cases, theoretical insights have been transferred into numerical algorithms through direct collaboration with computer scientists. This brought a bi-directional impacts where (i) mathematics boosts the progress in computation and (ii) computer science also helps mathematics. Simultaneously, fiber topology has been applied for decision making with multiple optimization problems.

The organizing board is now confident in adapting the achieved theories and techniques for industrial and inter-governmental decision making. We have conducted discussions with world-leading research groups to identify mutual interests that would advance both the society and techniques. With the proposed meeting, we finish the initial goal setting phase, and move on to the mission of providing solutions to application problems.

The meeting aids the interaction among mathematics, computation, and applications. For this, participants gather from broad spectra of research disciplines, including not only mathematics and computer science, but also operational research, sciences for environmental and semiconductors.

The operational research, led by Naoki Hamada (KLab), Daisuke Sakurai (Kyushu University Pan-Omics Data-Driven Research Innovation Center) and Takahiro Yamamoto (Tokyo Gakugei University) aims at designing benchmark problems for multioptimization problems utilizing knowledge extracted from fiber topology.

Environmental scientists Hiroshi Yamashita and Bastian Kern (German Aerospace Center, Germany) have some history of joint-research with Sakurai while he was at Zuse Institute Berlin (Germany). The current research project focuses on proposing a new tax incentive for balancing the environmental costs against the operational cost in the aviation industry. Fiber topology is employed for understanding the high-dimensional space spanned by different kinds of subcosts.

Finally, the application in semiconductor research employs fiber topology for understanding the potential fields of atomic configurations. For simulation outputs done with Japan's next-generation supercomputer Fugaku, we extract the landscape of the high-dimensional potential fields. Fiber topology gives a concise and parameter-free representation of the landscape, which is also robust against numerical errors.

All of the applications pose a challenge to the current state-of-the-art analysis of fiber topology. Especially, the high spatial dimensionality in the data is something that requires an update to the numerical methods. The current, rather loose, mathematics found in the computer science literature meets a more rigorous treatment by Takahiro Yamamoto (Tokyo Gakugei University).

Theorists not only provide solutions, but get feedback about desirable expansions. We discuss how fiber topology should let us extract information about the energy potential of atomic configurations, robustness of the assembly schedule against errors, and the impact of the inter-governmental decisions towards the aviation industry and air pollution.
While our progress in computation has seen a success, there are theoretical questions left, such as how the mathematical results translate to and from numerical representations.
What directions in mathematical theories benefit numerical ones, and vice versa, is another question.

The forum was co-sponsored by IMI and Pan-Omics Data-Driven Research Innovation Center. It was also supported by Kyushu University Kasseika project (令和2年度九州大学活性化制度).

Contents

九州大学 IMI 共同利用・研究集会（Ⅱ）

Fiber Topology Meets Applications

日時：　2021年1月6日（水）14:30 ～ 2021年1月8日（金）16:45
場所：　九州大学 伊都キャンパス ウエスト1号館 D棟4階
IMIオーディトリアム(W1-D-413)
※Zoomミーティングを使用したハイブリッド型で開催されます
https://www.imi.kyushu-u.ac.jp/kyodo-riyo/research_meetings/view/13

▶下記URLより参加登録をお願いいたします
https://forms.gle/EBEQP7VjivtienPEA

1月6日（水）

14:30-15:15
Title：Fiber Topology Meets Applications: Where We are Heading
Speaker：Daisuke Sakurai (Kyushu University)

15:15-16:00
Title：Why Topology is Necessary at Exascale - And Why it's Not Easy
Speaker：Hamish Carr (University of Leeds)

16:00-16:45
Title：Modeling semiconductor epitaxy for next generation power device application
Speaker：Yoshihiro Kangawa (Kyushu University)

1月7日（木）

14:30-15:15
Title：Data Parallel Hypersweeps for in Situ Topological Analysis
Speakers：Petar Hristov (University of Leeds), Gunther Weber (Lawrence Berkeley National Laboratory and University of California, Davis), Hamish Carr (University of Leeds), Oliver Rübel (Lawrence Berkeley National Laboratory) and James Ahrens (Los Alamos National Laboratory)

15:15-16:00
Title：Design of Multimodal Test Problems in Multiobjective Optimization Using Fiber Topology
Speakers：Reiya Hagiwara (Kyushu University), Naoki Hamada (KLab Inc.), Takahiro Yamamoto (Tokyo Gakugei University), Daisuke Sakurai (Kyushu

University)

16:00-16:45
Title : Eco-efficient Flight Trajectory Exploration by Using the Chemistry-climate Model EMAC
Speakers : Hiroshi Yamashita and Bastian Kern (German Aerospace Center)

1月8日（金）

14:30-15:15
Title : Elimination of B2 singularities
Speaker : Takahiro Yamamoto (Tokyo Gakugei University)

15:15-16:00
Simplifying Indefinite Fibrations on 4-manifolds
Speaker : Osamu Saeki (Kyushu University)

16:00-16:30
Title : An Efficient Triangulation for Extruded Spatiotemporal Prism Meshes
Speakers : Akito Fujii, Kenji Ono and Daisuke Sakurai (Kyushu University)

16:30-16:45
Concluding Remarks
Daisuke Sakurai (Kyushu University)

Fiber Topology Meets Applications: Where We Are Heading

Daisuke Sakurai

Kyushu Univ
2020 January 6

Thanks For Joining!

- We Are From
  - Math (Singularity Theory)
  - CompSci (Visualization)
  - Application Areas (Materials, Gaming, Atmosphere)

2

Thanks For Joining!

- Mutual Interest in
  - Topology of Fibers, eg
    - Configuration of
      - Local Extrema
      - Energy Landscapes

3

Thanks For Joining!

- Share Information
- Co-design Future Research

4

Topology in Visualization

- Algorithms (Hamish Carr, Shigeo Takahashi, S, …)
- Theories (Osamu Saeki, Takahiro Yamamoto, …)
- Collaboration (~2010)

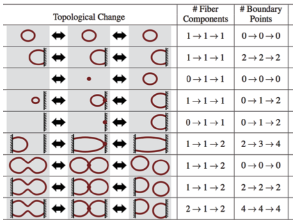

Inverse Images in 3D -> 2D maps

[Saeki & Yamamoto 2016]

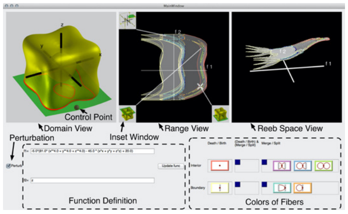

[S, Carr, Saeki… IEEE TVCG 2016]

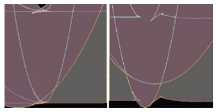

[Saeki, Takahashi, S,… 2014]

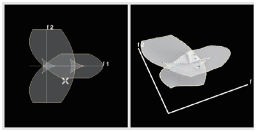

[S & Yamamoto 2019]

Vis for Math

Fiber = Inverse Image

Space-Time **Measurements**

$$f : R^n \to R^m$$

$f : R^2 \to R^1$

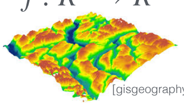

[gisgeography.com]

f^{-1} : Contours (コンタ) ⊂ Fibers

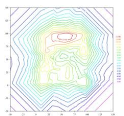

$f : R^3 \to R^1$

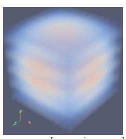

[paraview.org]

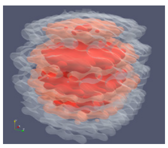

$f : R^3 \to R^m$

(Multi-Fields)

Fibers: $f^{-1}(f_1, f_2)$

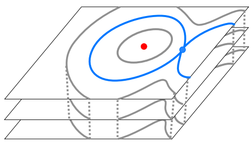

Contour Tree:
Compactifies Landscape

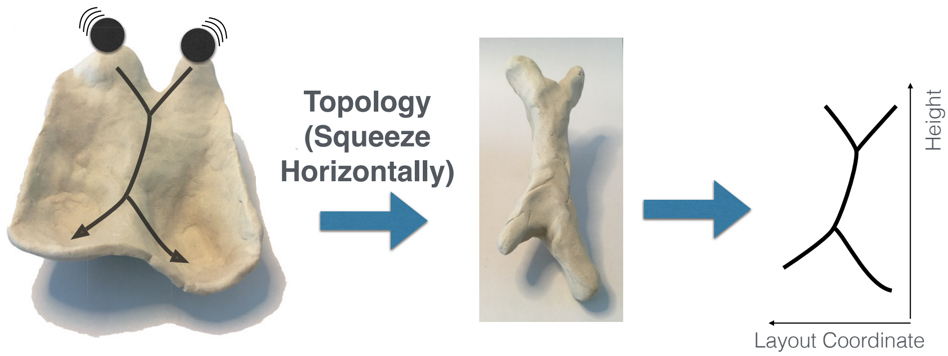

$f : R^2 \rightarrow$ **Height**

Contour Tree

7

Contour Trees For Visual Analysis

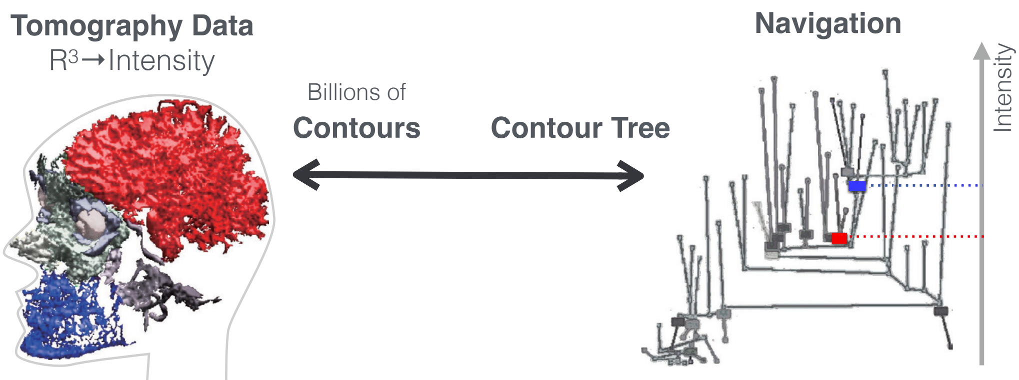

[Carr et al. 09]

8

Contour Tree for R^n

Eg with HC Hege, V Natarajan & M Weber

Toy Model

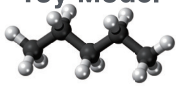

Conformation

16 Atoms
$=R^{16x3}$ State Coordinates

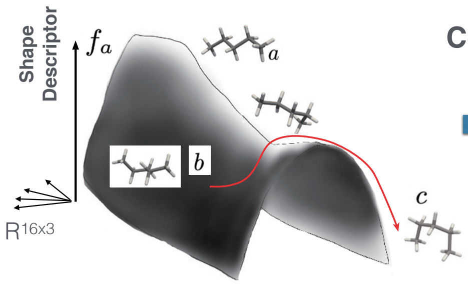

Contour Tree

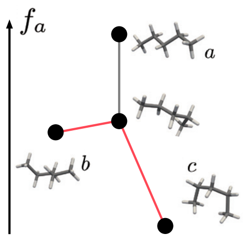

9

Reeb Space:
Compactifies Multi-Value *Landscape*

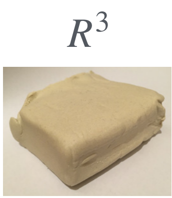

f →

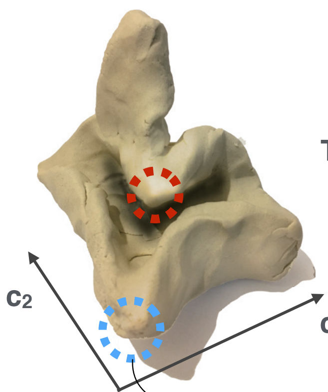

Topological "Squeeze"

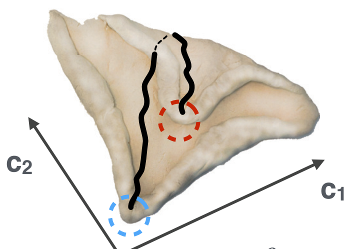

Reeb space of f

10

Math Development (O Saeki)

- Understand Fibers

→ Reliable Algorithms

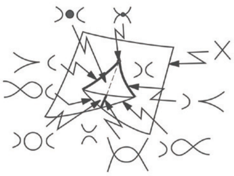

Classification & Configuration of Fibers, Morphs of Maps, …

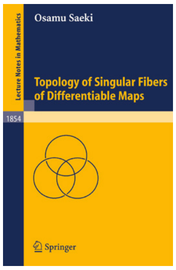

[Saeki 2004]

11

Timeline

- Algorithms
  - H Carr et al, ’00: Rn→R1
  - H Edelsbrunner et al, ’08: Idealized, Rn→Rm
  - H Carr & D Duke, ’13: Quantized Approximation
  - J Tierny & H Carr, ’17: R3→R2, Geometrical Impl.
  - Sakurai & H Carr (In Progress): Rn→R2, Combinatorial Impl.(?)
- Applications of Rn→R2
  - For Multiobjective Optimization (with N Hamada, T Yamamoto & R Hagiwara)
  - For Molecule Confirmation (with HC Hege & M Weber)

12

Coordinate Research Directions

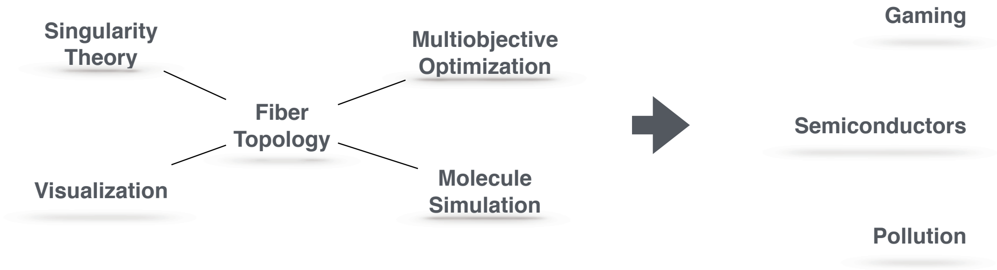

13

Don’t Forget

- Granted by IMI Kyodo Riyo
- Please acknowledge the funding accordingly

14

Why Topology Is Needed … And Why It's Not Easy

Hamish Carr

UNIVERSITY OF LEEDS

Overview

- I. Motivation
- II. Mathematics of Visualisation
- III. Topological Visualisation
- IV. Combinatoric Reduction
- V. Serial Contour Tree Algorithm
- VI. Challenges in Parallel

UNIVERSITY OF LEEDS

Data Is Increasing to Exascale

Fugaku:
7.6M cores
442 TFlops
1.77 EB/s

Summit:
2.4M cores
148 TFlops
0.59 EB/s

TaihuLight:
10.6M cores
93 TFlops
0.37 EB/s

Human Bandwidth Is Not

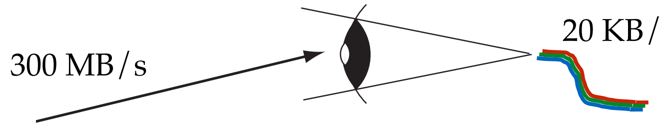

Topology

UNIVERSITY OF LEEDS

Optic Throughput

- 20KB 1s
- 1MB 50s ~ 1 m
- 1GB 50,000s ~ 13.9h
- 1TB 50,000,000s ~ 1.5y
- 1PB 50,000,000,000s ~ 1,500y
- 1EB 50,000,000,000,000s ~ 1,500,000y

Topology

UNIVERSITY OF LEEDS

A Visualisation Challenge

- 1 EB of data feasible (10^{18})
- 1 GB limit to comprehension (10^{9})
- 9 orders of magnitude (10^{-9}) data reduction
  - More if possible
- Visualisation turns into analysis
  - Domain-specific or domain-independent
  - Almost always based on mathematics

UNIVERSITY OF LEEDS

Level Sets (Contours)

- A *level set* is the inverse image of an *isovalue*

$$f^{-1}(h) = \{x \in \mathbb{R}^2 : f(x) = h \in \mathbb{R}\}$$

- A *contour* is a single connected component

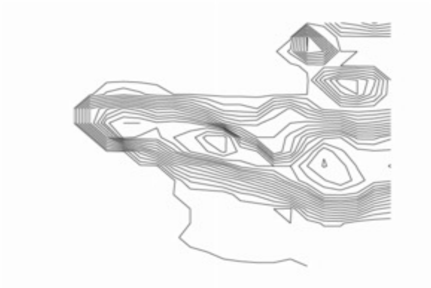

Contour Lines (2D)

Isosurfaces (3D)

UNIVERSITY OF LEEDS

Contours to Fibers

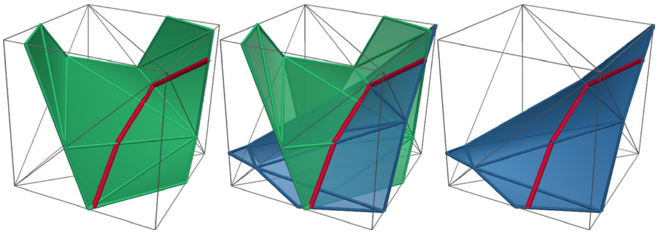

- Level sets of a point in range

$$f^{-1}(h) = \{x \in \mathbb{R}^3 : f(x) = h : h \in \mathbb{R}\}$$

- Intersection of isosurfaces of two functions

$$f^{-1}(h) = f_1^{-1}(h_1) \bigcap f_2^{-1}(h_2) : h = (h_1, h_2) \in \mathbb{R}^2$$

Topology

UNIVERSITY OF LEEDS

Fiber Surfaces

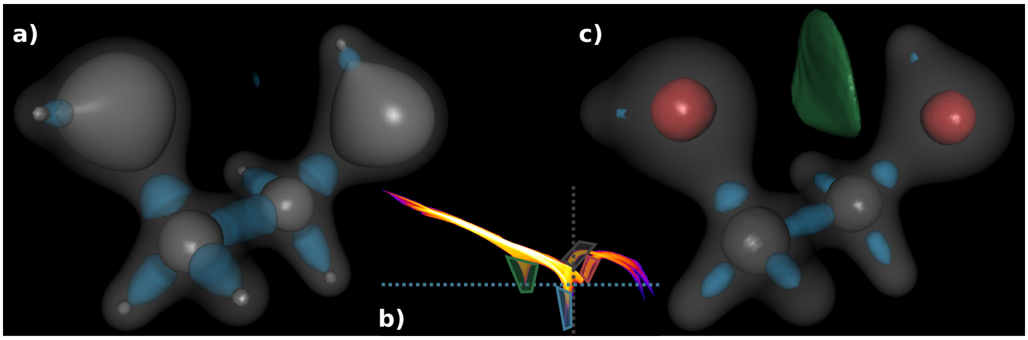

- Inverse image of a *curve*
- Provides surfaces for visualization

Topology

UNIVERSITY OF LEEDS

Streamlines to Gradient Lines

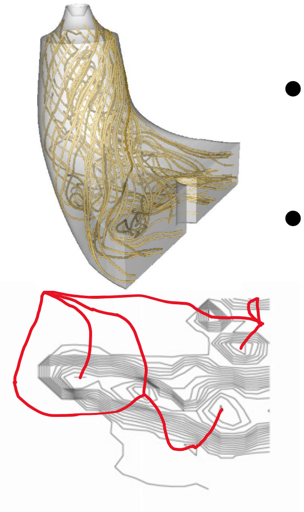

- Streamlines are tangent to a vector field
  - $\frac{\partial c}{\partial t} = \vec{f}(t)$
- Gradient lines are tangent to the gradient field
  - Always start at a *source* (max)
  - And end at a *sink* (min)
  - Perpendicular to the contours

Topology

UNIVERSITY OF LEEDS

Scientific Visualization

Scalar Field	Vector Field	Multi Field
$f:\mathbb{R}^d \rightarrow \mathbb{R}^1$	$f:\mathbb{R}^d \rightarrow \mathbb{R}^d$	$f:\mathbb{R}^m \rightarrow \mathbb{R}^n$

Isosurfaces
(Level Sets)

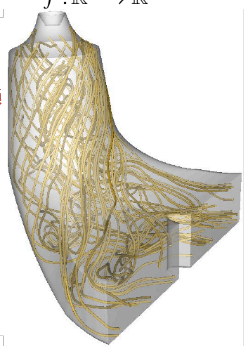

Streamlines

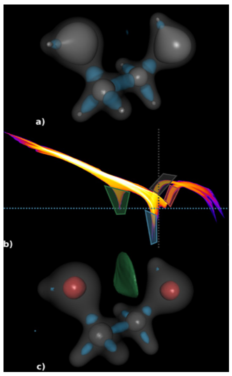

Fiber Surfaces

Topology

UNIVERSITY OF LEEDS

Selection

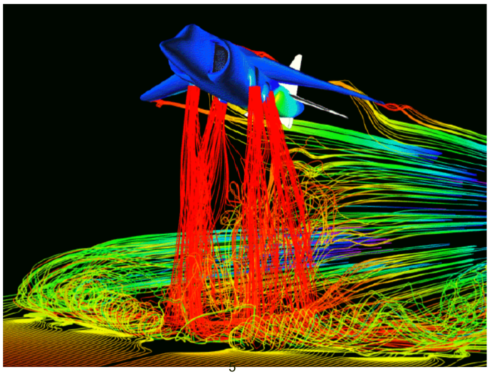

http://cs.swan.ac.uk/~csbob/teaching/csM07-vis/

- How do we *choose* what to visualise?

Topological Visualisation

- Analyse the data topologically
- Then use the analysis to identify features
- And show them to the user
- Or use them for later processing
- Ultimately, use them for decision-making
- More precisely, topology reduces the data size
- And allows selection among the features to do the same

The Contour Tree

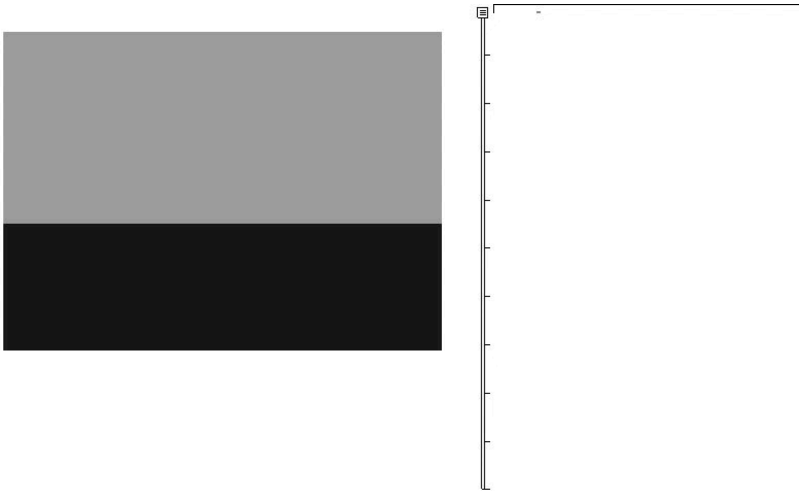

Topology

UNIVERSITY OF LEEDS

A 3D Contour Tree

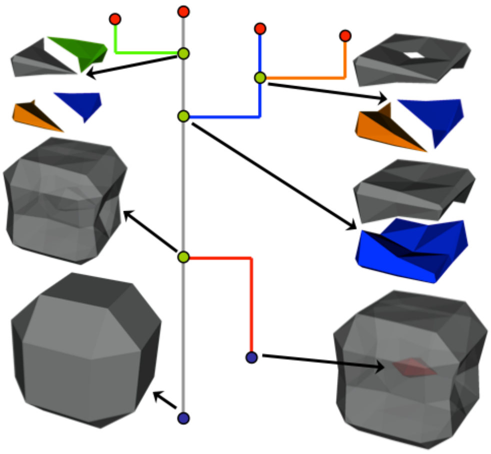

Colours:
Branch Decomposition
(Hierarchy of Features)

Hierarchy Induced by
Persistence
(isovalue range)

Topology

UNIVERSITY OF LEEDS

Indirect Manipulation

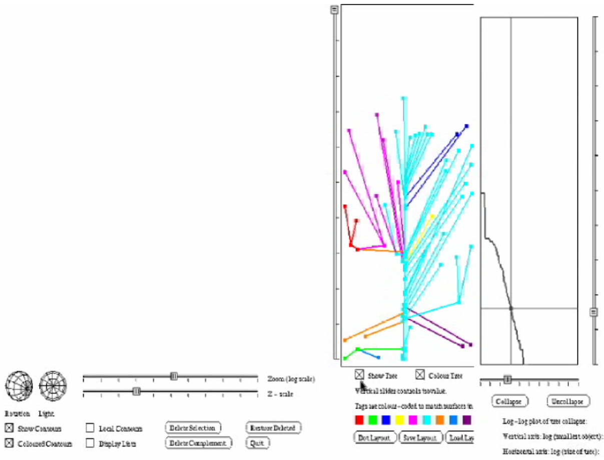

UNIVERSITY OF LEEDS

Topology

Feature Analysis

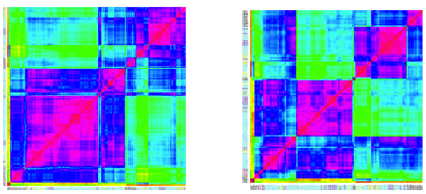

Protein Comparison
Zhang, Bajaj & Baker, 2004

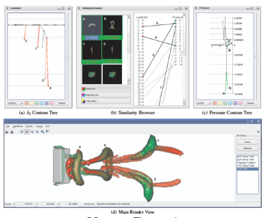

Vortex Detection
Schneider et al., 2008

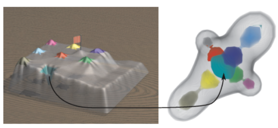

Fig. 9. Methane dataset: with average volume-to-area projection error of 1.5%. (Left) Topological landscape. (Right) Volume rendering using the same color scheme.

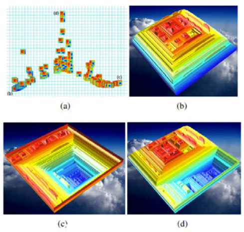

Energy Landscapes
Weber et al., 2007
Harvey & Wang 2010

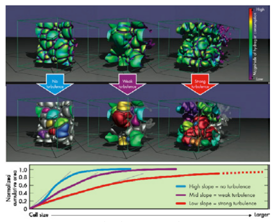

Turbulent Combustion
Bremer et al., 2009

UNIVERSITY OF LEEDS

Topology

The Reeb Graph

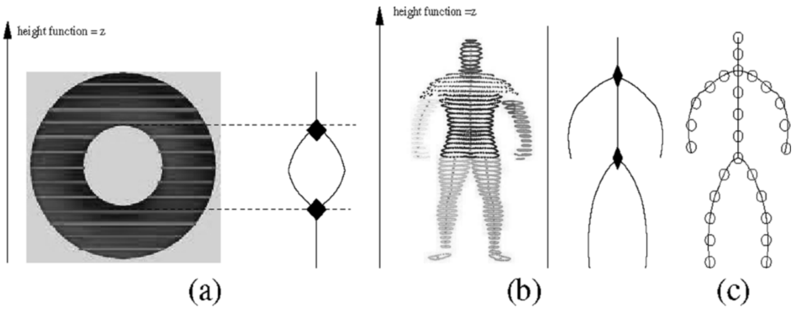

from Werghi, Xiao & Seibert, IEEE TSMC 2005

- For functions on manifolds
- Continuous contraction of contours
- Contour tree is a special case

Reeb Space

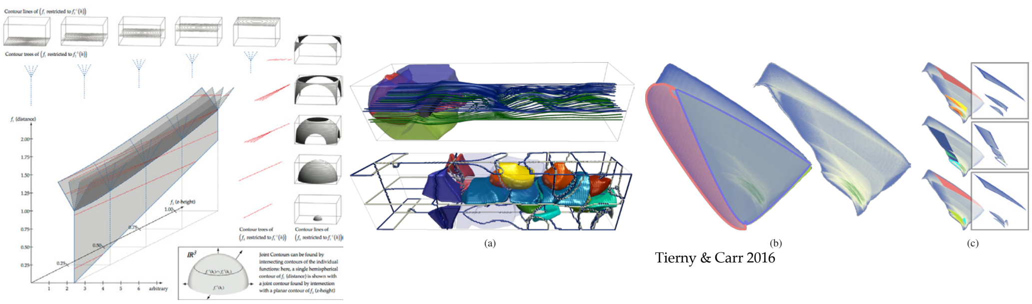

- Contract *fibers* not contours
- Quotient space built up from sheets, not edges
- Sheets have common behaviour – i.e. features

Morse-Smale Complex

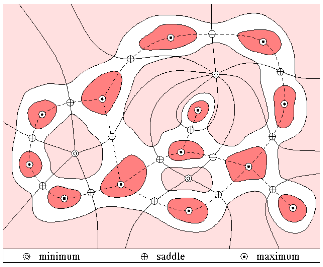

from Edelsbrunner et al., SCG 2001

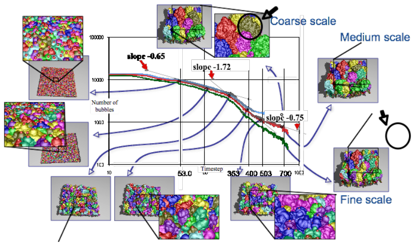

Oil/Liquid Mixing
Laney et al., Vis 2006

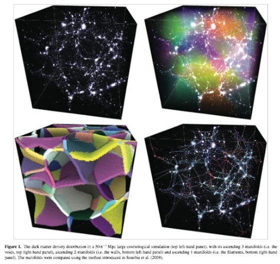

Cosmological Voids
Sousbie, 2011

- Based on Morse Theory
- Equivalence classes of gradient lines
- Divide space into features

Vector Topology

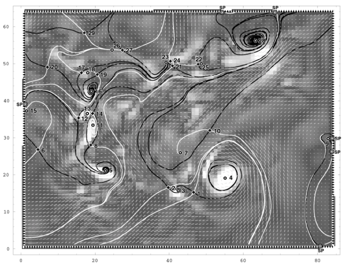

Hurricanes
Wong et al., 2001

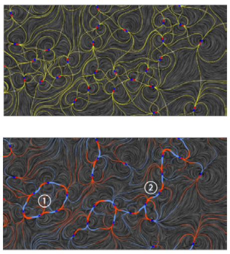

Magnetic Monopoles
Bachthaler et al., 2012

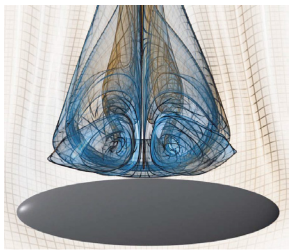

Vortex Breakdown
Hummel et al., 2011

- Based on vector analysis
- Equivalence classes of stream lines
- Features bounded by *separatrices*

Combinatorial Reduction

- Our analysis uses continuous mathematics
- Our computers use discrete mathematics
- We rely on mathematical simplifications:
  - Meshes, particles, &c. to discretise the mathematics
  - Numerics to compute the fields
  - Filtrations to enforce sequence
    - Most commonly, filtration by function value

Merge Tree Computation

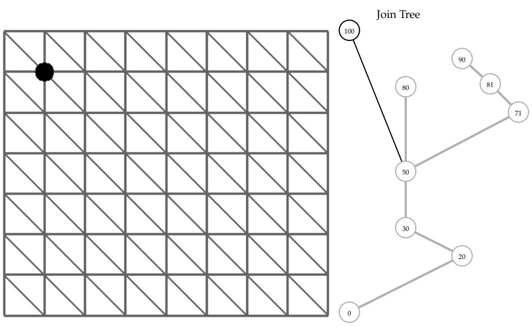

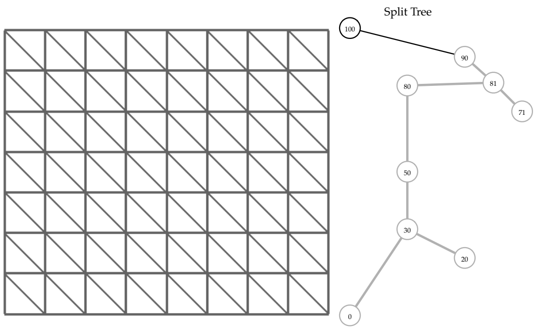

- Connectivity of $\{x: f(x) \geq h\}$
- Represented as *join* tree
- Sorting establishes a filtration

- Connectivity of $\{x: f(x) \leq h\}$
- Represented as *split* tree
- Reversed filtration

UNIVERSITY OF LEEDS

Transfer Phase

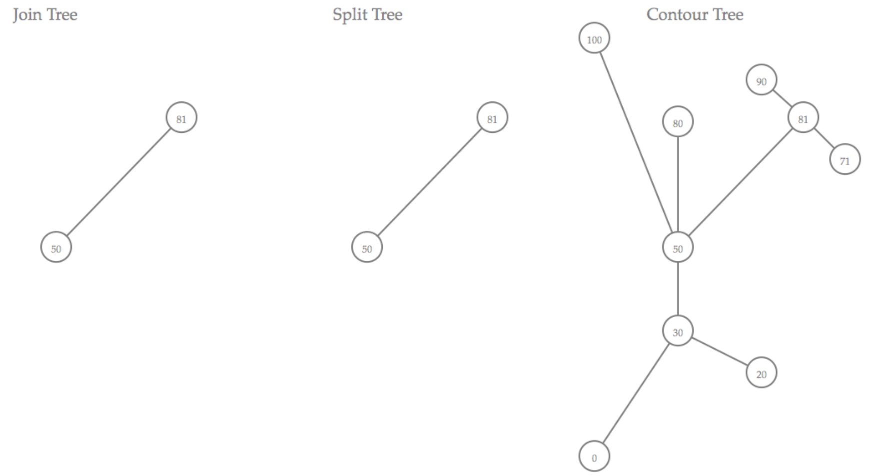

Topology

UNIVERSITY OF LEEDS

Simplification / Branch Decomposition

- Large trees have millions of edges
- So we prune edges in sequence
- With importance measure
- Results in a branch decomposition

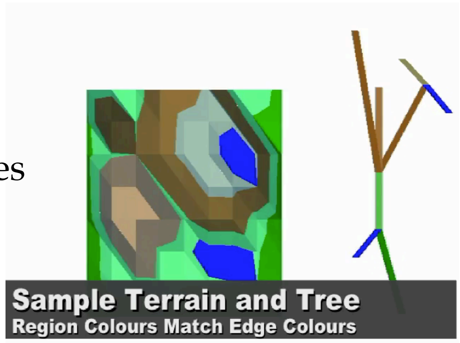

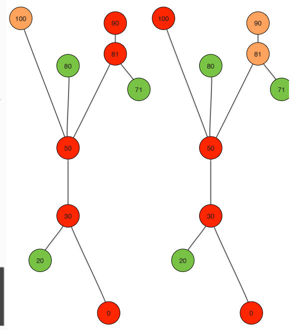

Area Height

Topology

UNIVERSITY OF LEEDS

Serial vs. Parallel

- Filtrations usually process data in sequential sorted order
- We add edges to the tree one at a time
- Simplification is one edge at a time
- Proofs use linear induction
- So the big question is:
  - How do we scale up to parallel systems?
  - Petar will discuss this tomorrow

Topology

UNIVERSITY OF LEEDS

Acknowledgements

- NSERC
- University of British Columbia
- SFI
- University College Dublin
- EPSRC EP/J013072/1
- University of Leeds
- DoE/NNSA ECP Alpine 17-SC-20-SC LBNL Subcontract 7452335

Topology

UNIVERSITY OF LEEDS

Jan. 6, 16:00-16:45

Modeling semiconductor epitaxy for next generation power device application

Yoshihiro KANGAWA[1, 2]

[1] RIAM, Kyushu University, Japan
[2] IMaSS, Nagoya University, Japan

Renewable Energy Materials Engineering

Acknowledgements

1. MEXT GaN R&D Project (Grant Number JPJ005357)
2. JSPS KAKENHI (Grant Number JP16H06418)
3. JST CREST (JPMJCR16N2)
4. JST SICORP (Grant Number 16813791B)
5. European Union's Horizon 2020 research and innovation program (Grant Number 720527: InRel-NPower project)

https://sites.google.com/view/kangawalab/

GaN MOVPE (Metal-Organic Vapor Phase Epitaxy)

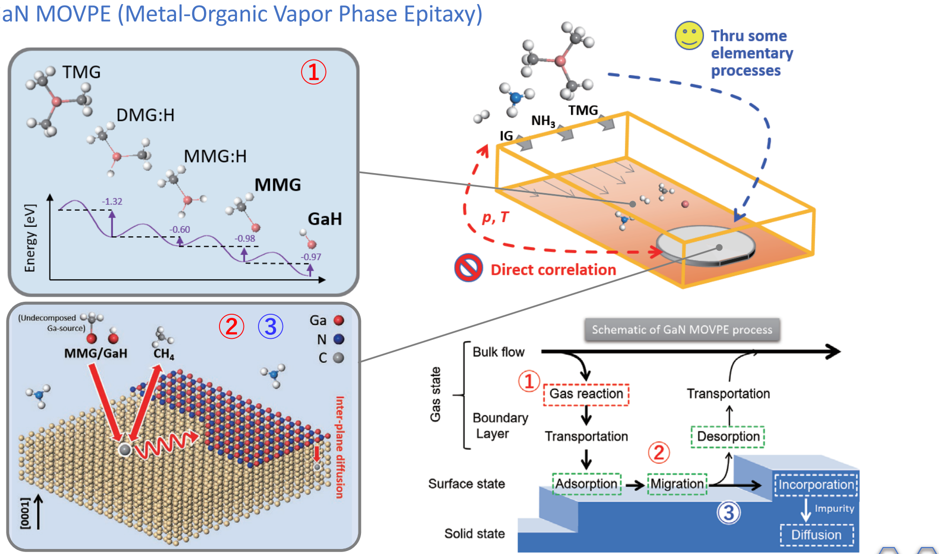

Yoshihiro Kangawa (Kyushu Univ.)

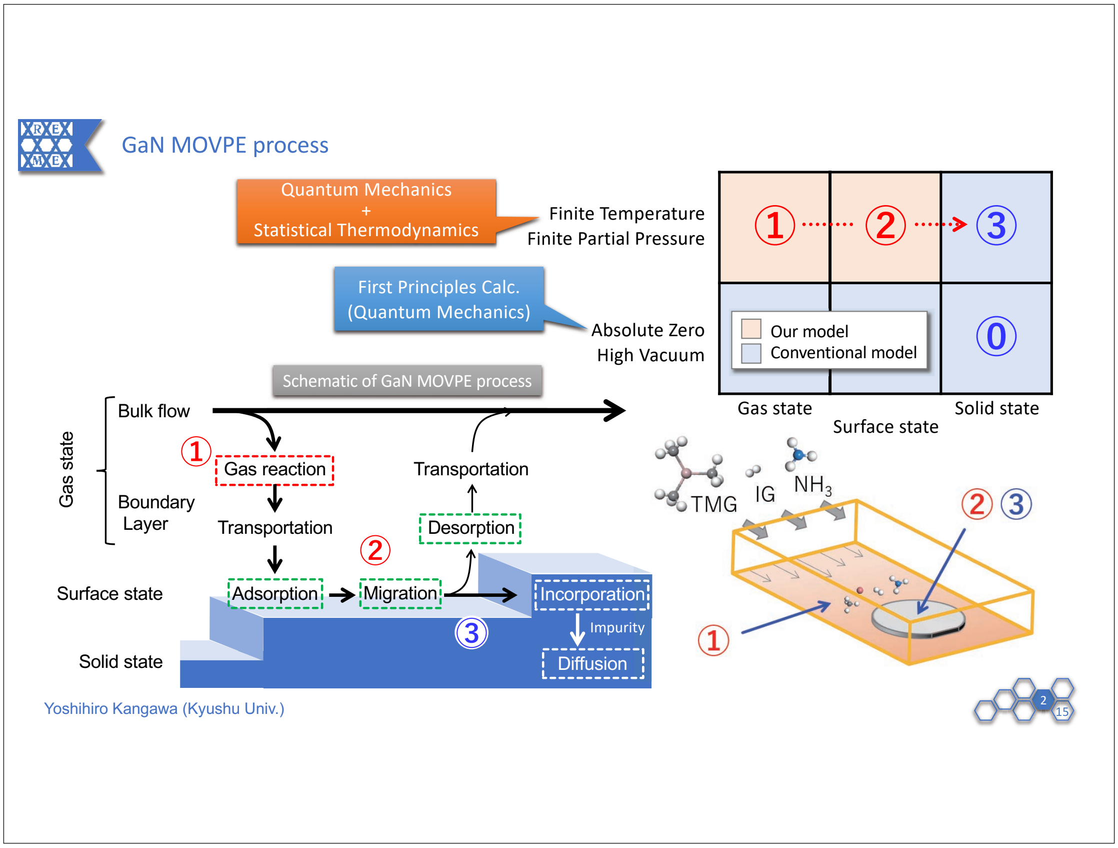
GaN MOVPE process
Quantum Mechanics + Statistical Thermodynamics
Finite Temperature
Finite Partial Pressure
First Principles Calc. (Quantum Mechanics)
Absolute Zero
High Vacuum
① ② ③
Our model
Conventional model
0
Gas state
Surface state
Solid state
Schematic of GaN MOVPE process
Gas state
Bulk flow
Boundary Layer
① Gas reaction
Transportation
Transportation
Desorption
②
Surface state
Adsorption
Migration
Incorporation
③
Impurity
Diffusion
Solid state
TMG
IG
NH_3
② ③
①
Yoshihiro Kangawa (Kyushu Univ.)
2
15

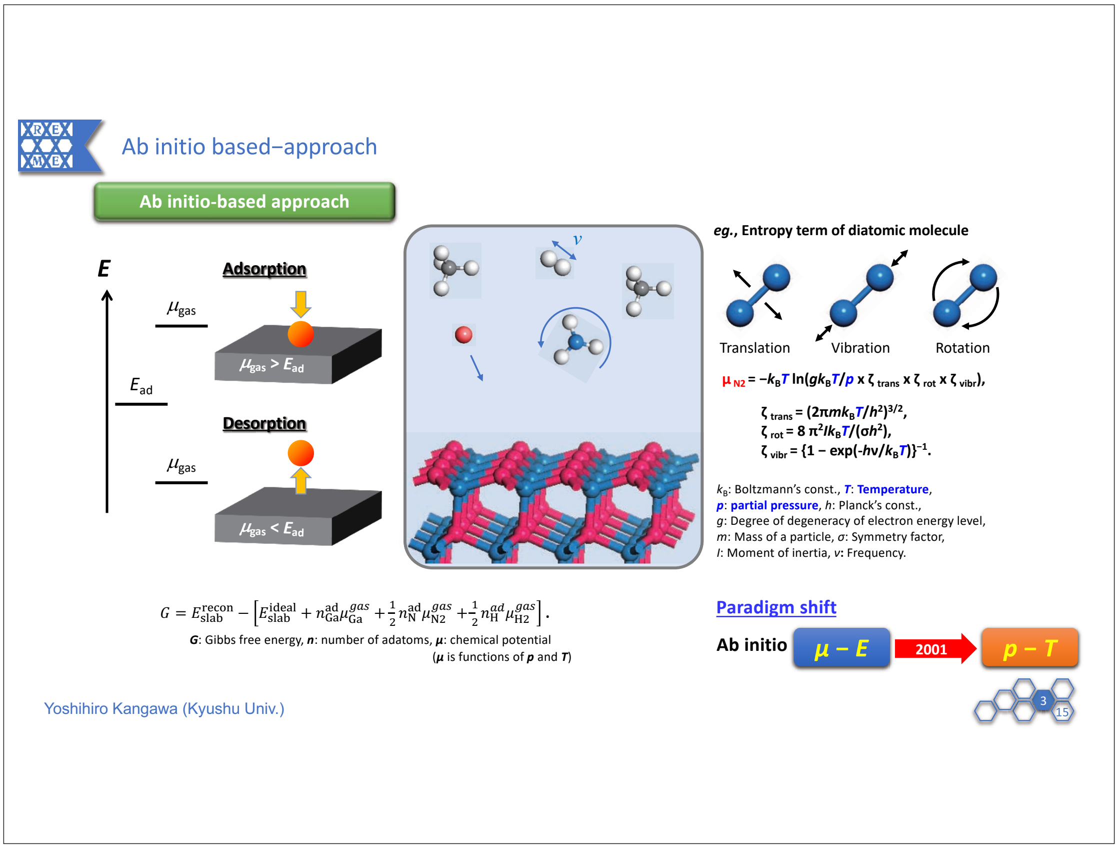
Ab initio based–approach
Ab initio-based approach
E
Adsorption
μ_{gas}
$\mu_{gas} > E_{ad}$
E_{ad}
Desorption
μ_{gas}
$\mu_{gas} < E_{ad}$
v
eg., Entropy term of diatomic molecule
Translation
Vibration
Rotation
$\mu_{N2} = -k_BT \ln(gk_BT/p \times \zeta_{trans} \times \zeta_{rot} \times \zeta_{vibr})$,
$\zeta_{trans} = (2\pi m k_BT/h^2)^{3/2}$,
$\zeta_{rot} = 8\pi^2 I k_BT/(\sigma h^2)$,
$\zeta_{vibr} = \{1 - \exp(-hv/k_BT)\}^{-1}$.
k_B: Boltzmann's const., T: Temperature,
p: partial pressure, h: Planck's const.,
g: Degree of degeneracy of electron energy level,
m: Mass of a particle, σ: Symmetry factor,
I: Moment of inertia, v: Frequency.
$G = E_{slab}^{recon} - \left[E_{slab}^{ideal} + n_{Ga}^{ad}\mu_{Ga}^{gas} + \frac{1}{2}n_N^{ad}\mu_{N2}^{gas} + \frac{1}{2}n_H^{ad}\mu_{H2}^{gas}\right]$.
G: Gibbs free energy, n: number of adatoms, μ: chemical potential
(μ is functions of p and T)
Paradigm shift
Ab initio
$\mu - E$
2001
$p - T$
Yoshihiro Kangawa (Kyushu Univ.)
3
15

Multi-physics Crystal Growth Simulation

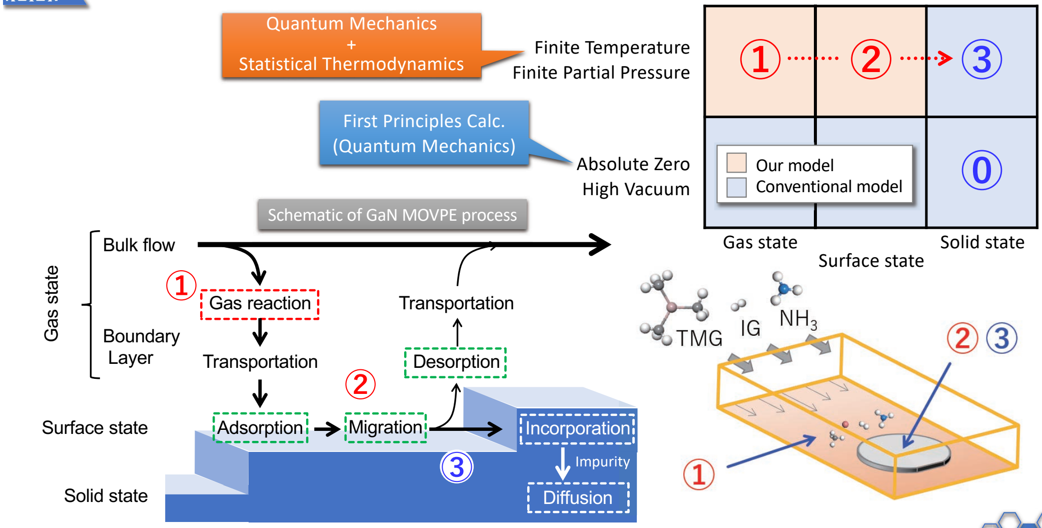

Yoshihiro Kangawa (Kyushu Univ.)

C incorporation in GaN MOVPE: Vapor phase reaction

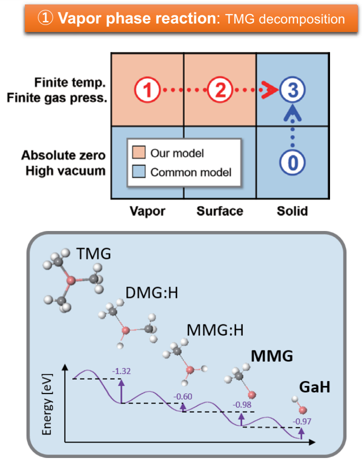

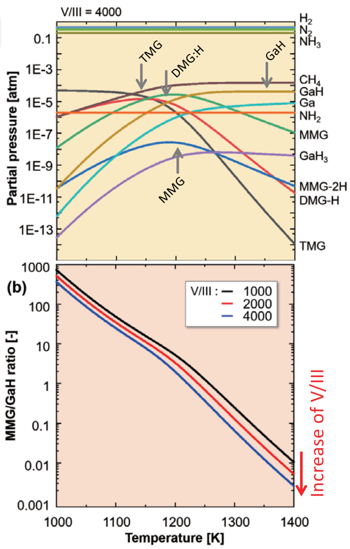

Y. Ohkawachi, 2019

Thermodyamic analyses
$\Sigma p^{eq} = 1\text{atm}$, V/III: 4000,
NH_3 input partial pressure$p^{eq}_{NH3} = 0.2$ atm,
NH_3→NH_2 decomposition rate $\alpha = 1.0\times10^{-5}$,
NH_3→N_2 decomposition rate $\beta = 1.0\times10^{-2}$,
Carrier gas: H_2 .

Equilibrium const.

$$K_1 = \alpha^2 \cdot \frac{p^{eq}_{DMGH} \cdot p^{eq}_{CH4}}{p^{eq}_{TMG}} \quad (1)$$

$$K_2 = \alpha^2 \cdot \frac{p^{eq}_{MMGH2} \cdot p^{eq}_{CH4}}{p^{eq}_{DMGH}} \quad (2)$$

$$K_3 = \frac{p^{eq}_{MMG} \cdot p^{eq}_{H2}}{p^{eq}_{MMGH2}} \quad (3)$$

$$K_4 = \alpha^2 \cdot \frac{p^{eq}_{GaH3} \cdot p^{eq}_{CH4}}{p^{eq}_{MMGH2}} \quad (4)$$

$$K_5 = \frac{p^{eq}_{GaH} \cdot p^{eq}_{H2}}{p^{eq}_{GaH3}} \quad (5)$$

$$K_6 = \frac{p^{eq}_{Ga} \cdot {p^{eq}_{H2}}^{1/2}}{p^{eq}_{GaH}} \quad (6)$$

Constraint condition

$$p^{eq}_{TMG} + p^{eq}_{DMGH} + p^{eq}_{MMGH2} + p^{eq}_{MMG} + p^{eq}_{GaH3} + p^{eq}_{GaH} + p^{eq}_{Ga} = Zp^{0}_{TMG} \quad (7)$$

$$3p^{eq}_{TMG} + 2p^{eq}_{DMGH} + p^{eq}_{MMGH2} + p^{eq}_{MMG} + p^{eq}_{CH4} = 3Zp^{0}_{TMG} \quad (8)$$

$$9p^{eq}_{TMG} + 7p^{eq}_{DMGH} + 5p^{eq}_{MMGH2} + 3p^{eq}_{MMG} + 3p^{eq}_{GaH3} + p^{eq}_{GaH} + p^{eq}_{Ga} + 4p^{eq}_{CH4} + 3p^{eq}_{NH3} + 2p^{eq}_{NH2} + 2p^{eq}_{H2} = Z\left(9p^{0}_{TMG} + 3p^{0}_{NH3} + 2p^{0}_{NH2} + p^{0}_{H2}\right) \quad (9)$$

$$p^{eq}_{TMG} + p^{eq}_{DMGH} + p^{eq}_{MMGH2} + p^{eq}_{MMG} + p^{eq}_{GaH3} + p^{eq}_{GaH} + p^{eq}_{Ga} + p^{eq}_{CH4} + p^{eq}_{NH3} + p^{eq}_{NH2} + p^{eq}_{H2} + p^{eq}_{N2} = p^{eq} = 1\text{atm} \quad (10)$$

Yoshihiro Kangawa (Kyushu Univ.)

C incorporation in GaN MOVPE: Surface reaction

② Surface reconstruction

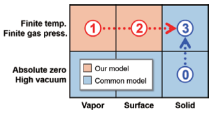

Representative surface models

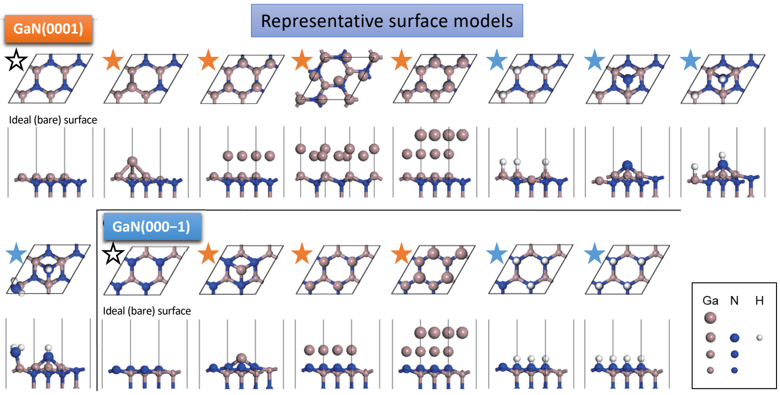

Evaluation criteria of stable surface reconstruction under a certain growth condition

$$G = E^{\mathrm{recon}}_{\mathrm{slab}} - \left[E^{\mathrm{ideal}}_{\mathrm{slab}} + n^{\mathrm{ad}}_{\mathrm{Ga}}\mu^{gas}_{\mathrm{Ga}} + \frac{1}{2}n^{\mathrm{ad}}_{\mathrm{N}}\mu^{gas}_{\mathrm{N2}} + \frac{1}{2}n^{ad}_{\mathrm{H}}\mu^{gas}_{\mathrm{H2}}\right].$$

G: Gibbs free energy, ***n***: number of adatoms, ***μ***: chemical potential
(***μ*** is functions of ***p*** and ***T***)

★ Ga-rich surface model
★ N–H-rich surface model

A. Kusaba et al., JJAP **56** (2017) 070304

Yoshihiro Kangawa (Kyushu Univ.)

6 / 15

C incorporation in GaN MOVPE: Surface reaction

② Surface reconstruction

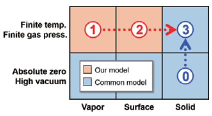

p^0_{tot} = 1 atm, p^0_{NH3} = 0.5 atm, α = 0.25, F = 0 or 1

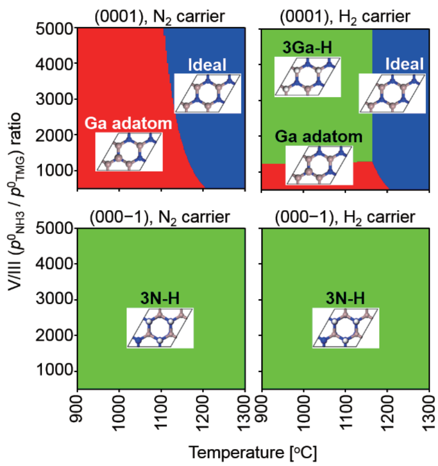

GaN(0001)

✓ Ga_{ad} surface is stable under N_2 carrier gas condition.

✓ 3Ga-H surface is stable under H_2 carrier gas condition.

GaN(000−1)

✓ 3N-H surface is stable under typical growth condition.

Yoshihiro Kangawa (Kyushu Univ.)

7 / 15

C incorporation in GaN MOVPE: Surface reaction

② Surface reaction

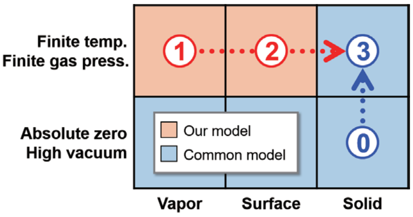

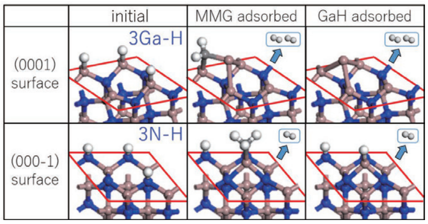

Carbon concentration on the growth surface

$$\rho_{C,\mathrm{surface}} = \rho_{N\text{-site}} \frac{p_{MMG} C_{s,MMG}}{p_{MMG} C_{s,MMG} + p_{GaH} C_{s,GaH}}$$

✓ P_i : Partial pressure of molecule *i*
✓ $C_{s,MMG}$: Adsorption probability of molecule *i*

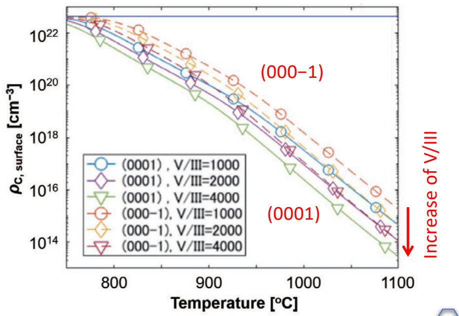

Yoshihiro Kangawa (Kyushu Univ.)

C incorporation in GaN MOVPE: Interlayer diffusion

③ Interlayer diffusion

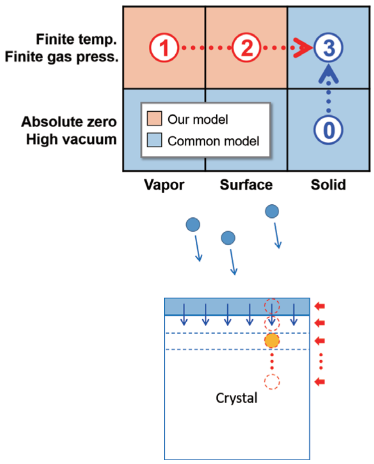

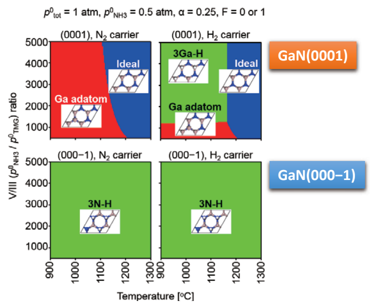

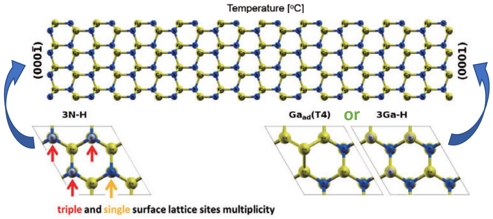

Yoshihiro Kangawa (Kyushu Univ.)

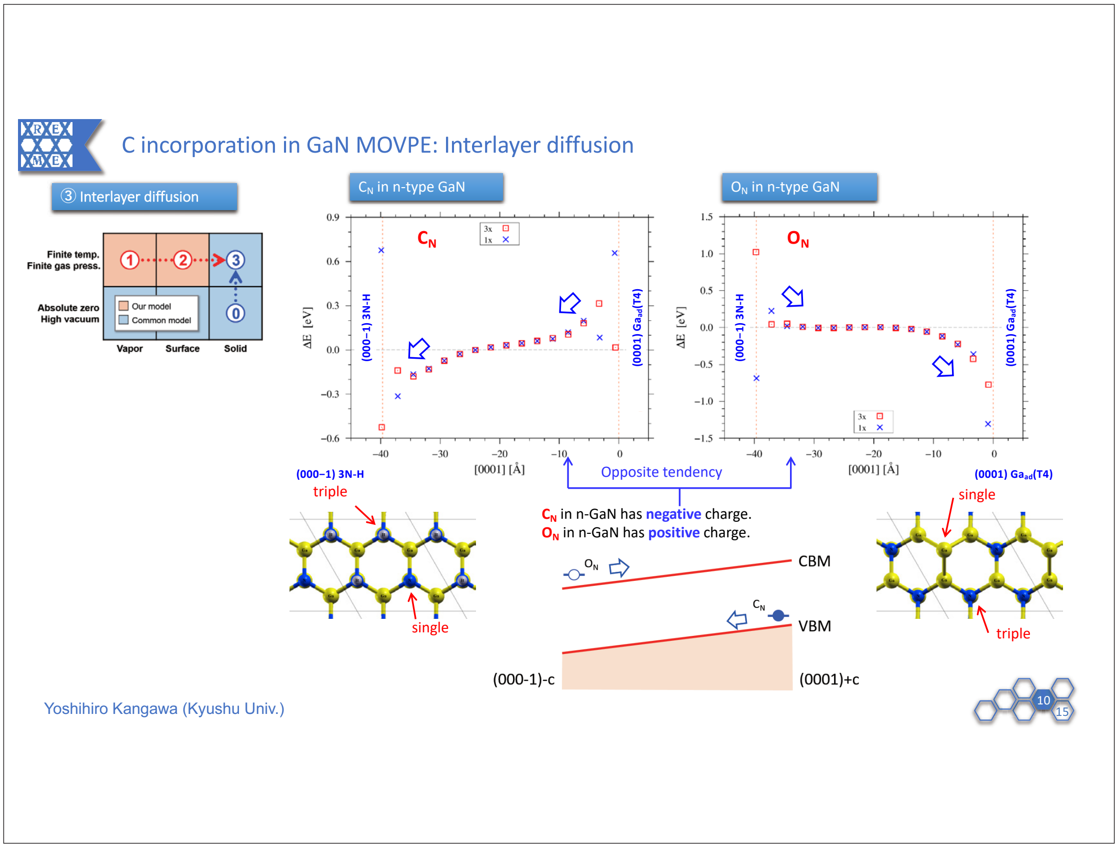

C incorporation in GaN MOVPE: Interlayer diffusion
③ Interlayer diffusion
Finite temp. Finite gas press.
Absolute zero High vacuum
Our model
Common model
Vapor
Surface
Solid
C_N in n-type GaN
O_N in n-type GaN
C_N
O_N
3x
1x
ΔE [eV]
[0001] [Å]
(000−1) 3N-H
(0001) Ga_{ad}(T4)
triple
single
Opposite tendency
C_N in n-GaN has negative charge.
O_N in n-GaN has positive charge.
CBM
VBM
(000-1)-c
(0001)+c
Yoshihiro Kangawa (Kyushu Univ.)
10
15

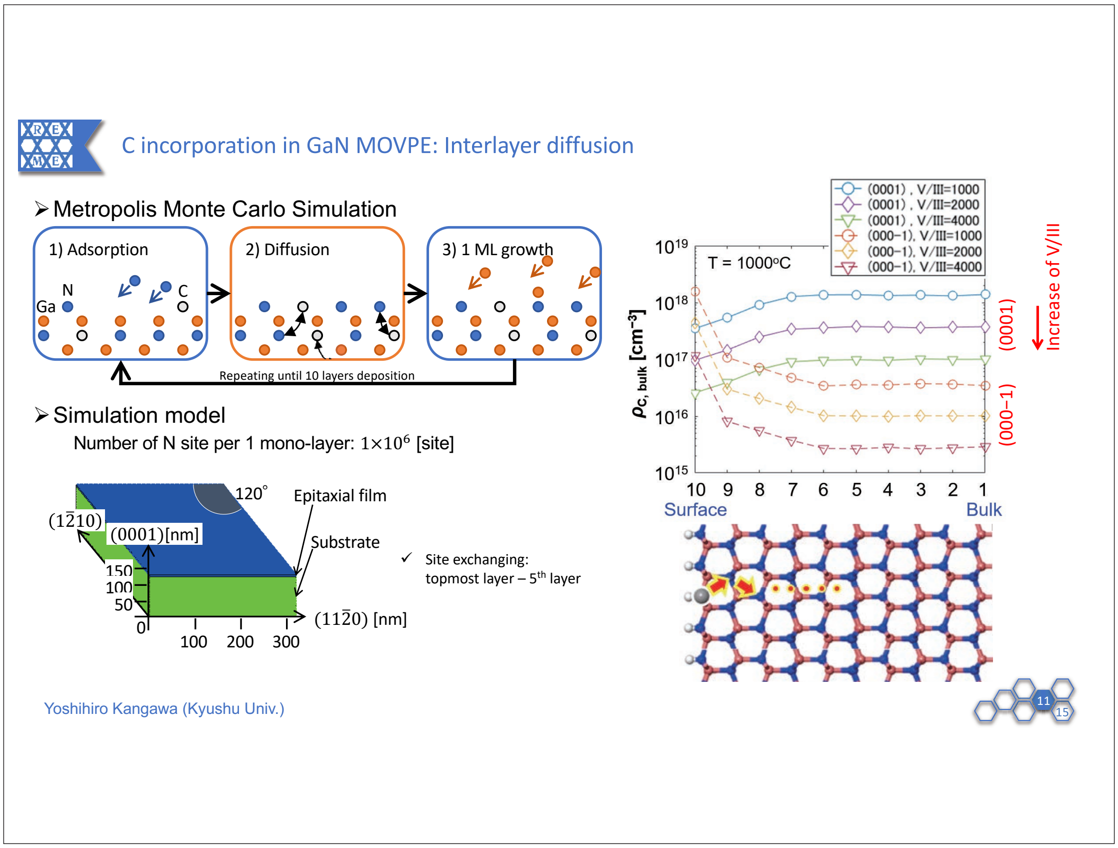

C incorporation in GaN MOVPE: Interlayer diffusion
➢ Metropolis Monte Carlo Simulation
1) Adsorption
2) Diffusion
3) 1 ML growth
Ga
N
C
Repeating until 10 layers deposition
➢ Simulation model
Number of N site per 1 mono-layer: 1×10^6 [site]
120°
Epitaxial film
Substrate
$(1\bar{2}10)$
(0001)[nm]
150
100
50
0
100
200
300
$(11\bar{2}0)$ [nm]
✓ Site exchanging: topmost layer – 5th layer
(0001), V/III=1000
(0001), V/III=2000
(0001), V/III=4000
(000−1), V/III=1000
(000−1), V/III=2000
(000−1), V/III=4000
T = 1000°C
$\rho_{C,\,bulk}$ [cm^{-3}]
10^{19}
10^{18}
10^{17}
10^{16}
10^{15}
10 9 8 7 6 5 4 3 2 1
Surface
Bulk
(0001)
(000−1)
Increase of V/III
Yoshihiro Kangawa (Kyushu Univ.)
11
15

C incorporation in GaN MOVPE: Integrated model

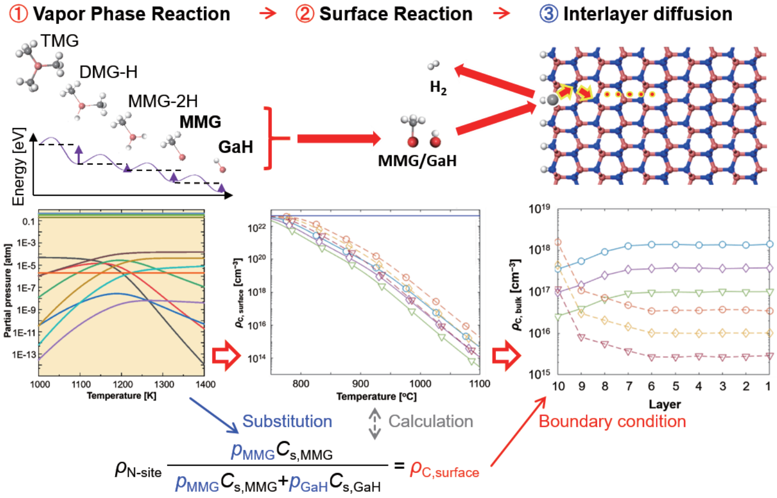

Yoshihiro Kangawa (Kyushu Univ.)

C incorporation in GaN MOVPE: Integrated model

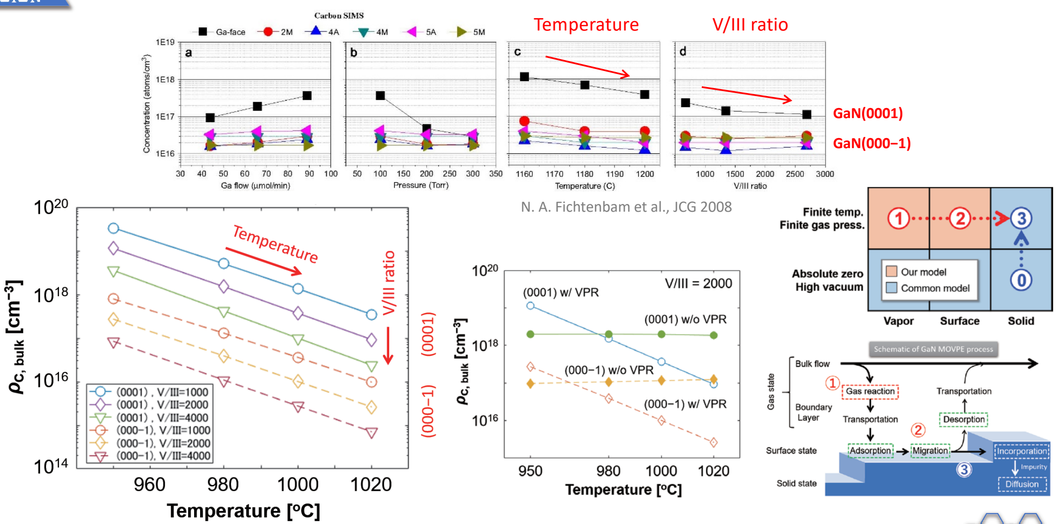

Yoshihiro Kangawa (Kyushu Univ.)

Summary

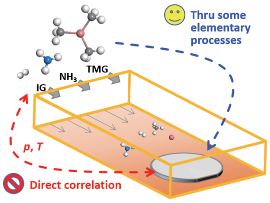

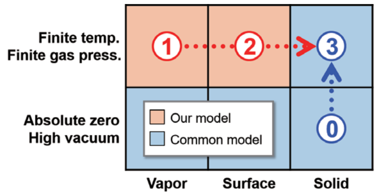

Experiments

Change in Growth conditions	Carbon concentration
Increase of Temperature	↓
Increase of V/III ratio	↓
Change in Growth Orientation: (0001) → (000−1)	↓

Yoshihiro Kangawa (Kyushu Univ.)

Summary

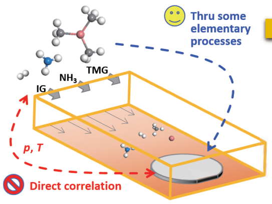

Integrated model

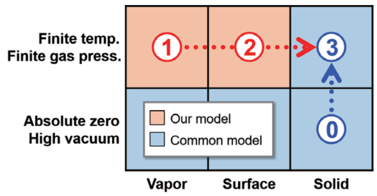

Change in Growth conditions	① Vapor Phase Reaction	② Surface Reaction	③ Interlayer diffusion	Carbon concentration
Input parameter	*Contribution of each elementary growth process*			*Resulting output*
Increase of Temperature	↓	↑	↑	↓
Increase of V/III ratio	↓	-	-	↓
Change in Growth Orientation: (0001) → (000−1)	-	↑	↓	↓

Yoshihiro Kangawa (Kyushu Univ.)

Data Parallel Hypersweeps for In Situ Computation

Petar Hristov
Gunther Weber
Hamish Carr
Oliver Ruebel
James Ahrens

UNIVERSITY OF LEEDS

Overview

1. In Situ Computation
2. Parallel Contour Tree Analysis
3. In Situ Contour Tree Pipeline

UNIVERSITY OF LEEDS

Visualization at Scale

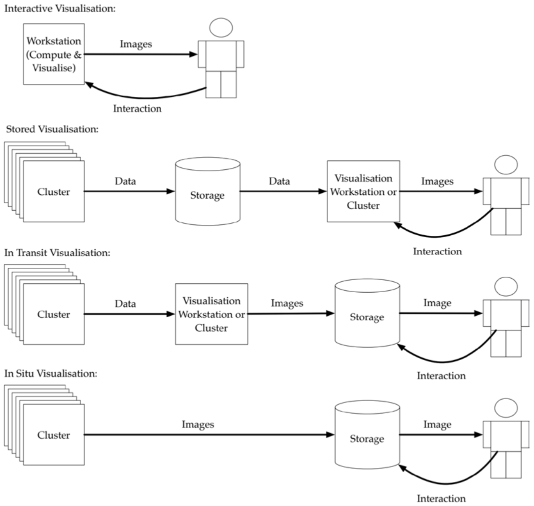

In Situ Visualization Summary

- Uses a supercomputer.
- Happens during data generation.
- Requires robust data reduction tools.
- Parallel and distributed algorithms are mandatory.

UNIVERSITY OF LEEDS

Evolution of Algorithms at Scale

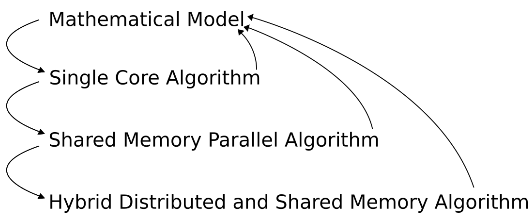

- Reeb Graph (1940s).
- Sweep and Merge Algorithm (2000s).
- Parallel Peak Pruning (2010s).
- Distributed Parallel Peak Pruning (2020s).

UNIVERSITY OF LEEDS

Parallel Algorithm Principles

- Use local independent operations.
- Rely on parallel primitives – test, scan, sort.
- Avoid synchronisation and global invariants.
- Avoid data transfers between devices.

UNIVERSITY OF LEEDS

Parallel Peak Pruning

- Instead of incremental computation
- Compute monotone paths in parallel
  - Essentially, up the gradient lines
- Use them to identify peaks
- Strip out *all peaks at once*
- Repeat recursively

UNIVERSITY OF LEEDS

An Ascending Forest

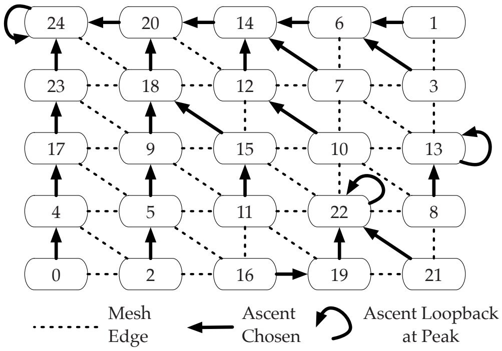

- Every vertex chooses *an* uphill neighbour
- Peaks loop back to themselves

UNIVERSITY OF LEEDS

Upwards Path Compression

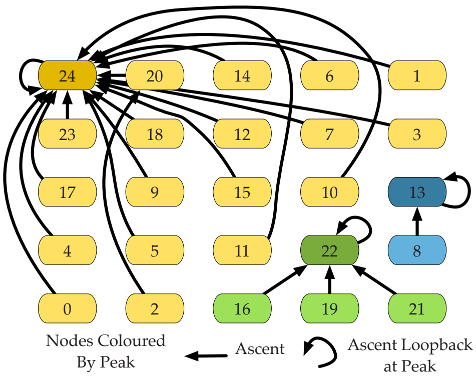

- Use pointer-doubling to compress paths
- Establishes peaks as roots in union-find

UNIVERSITY OF LEEDS

Saddle Candidates

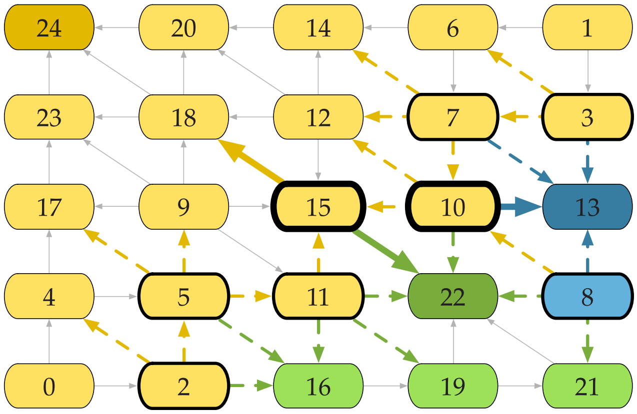

Nodes Coloured By Peak

Edges Coloured By Peak

Saddle Candidates in Bold

UNIVERSITY OF LEEDS

Governing Saddles

From Saddle Candidate	1	1	1	1	1	1	1	1	1	1	1	1	1	1	1	1	1	1	1	1
Peak for Upper End	24	24	24	24	24	24	24	24	24	24	24	24	24	24	24	22	22	22	22	22
Lower End	15	11	10	10	8	7	7	7	5	5	5	3	3	2	2	15	11	11	11	10

From Saddle Candidate	1	1	1	1	1	1	1	1	0	0	0	0	0	0	0	0	0	0	0	0
Peak for Upper End	22	22	22	22	13	13	13	13	24	24	24	24	24	24	24	24	24	24	24	24
Lower End	8	8	5	2	10	8	7	3	23	20	18	18	18	17	14	12	12	12	12	9

From Saddle Candidate	0	0	0	0	0	0	0	0	0	0	0	0	0	0	0	0
Peak for Upper End	24	24	24	24	24	24	24	24	24	24	24	24	22	22	22	22
Lower End	9	9	9	9	6	6	4	4	1	1	0	0	21	19	19	16

- Highest candidate is peak's *governing* saddle
- Found by sorting edges

UNIVERSITY OF LEEDS

Second Pass

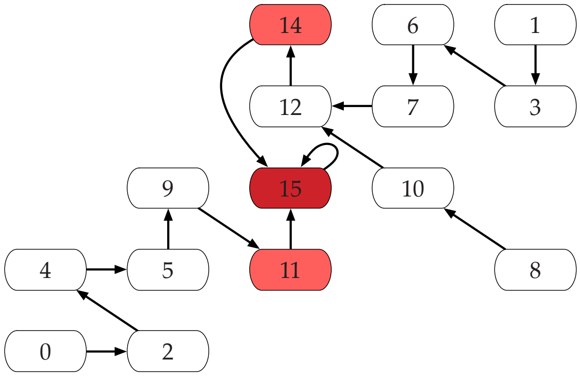

Ascents Chosen

- Single peak is base case for recursion

UNIVERSITY OF LEEDS

Contour Tree Phase

- Essentially the same as the serial
- But batched, alternating upper / lower leaves
- Vertex deletion is lazy: we set a flag
- Then use path compression to remove them
- This allows *parallel* transfer of leaves

UNIVERSITY OF LEEDS

Hyperstructure Idea

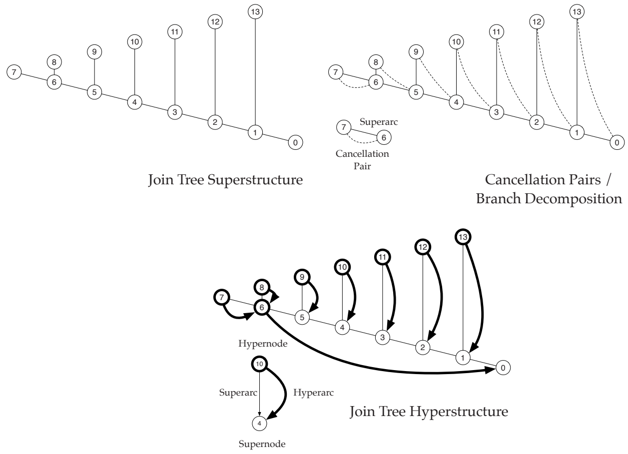

UNIVERSITY OF LEEDS

Simplification via Hypersweep

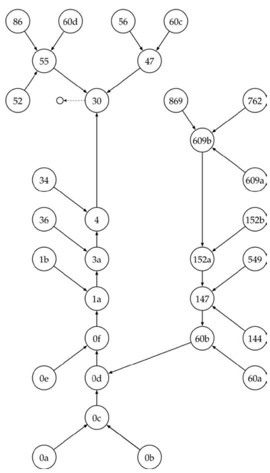

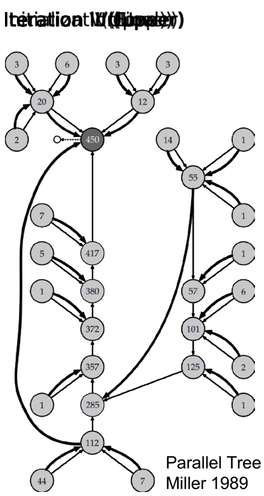

Parallel Tree Contraction
Miller 1989

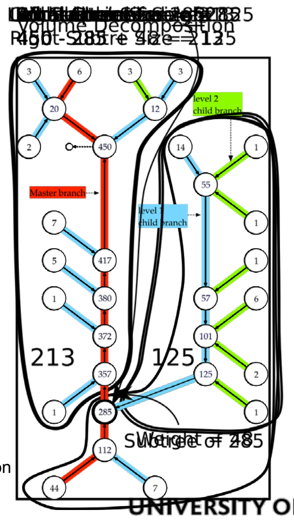

UNIVERSITY OF LEEDS

In Situ Visualization Pipeline

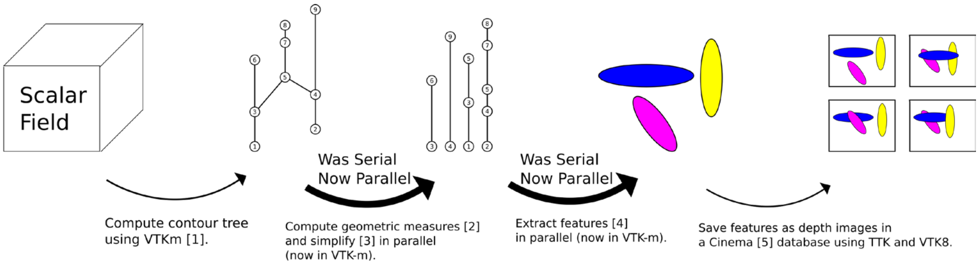

1. “Parallel Peak Pruning”, Carr et al. 2017
2. “Simplifying Flexible Isosurfaces with Local Geometric Measures”, Carr et al. 2004
3. “Multi-Resolution Computation and Presentation of Contour Trees”, Pascucci et al. 2004
4. “Topology-Controlled Volume Rendering”, Weber et al. 2007
5. “An Image-Based Approach to Extreme Scale in Situ Visualization and Analysis”, Ahrens et al. 2014

UNIVERSITY OF LEEDS

In Situ Pipeline - Feature Visualisation

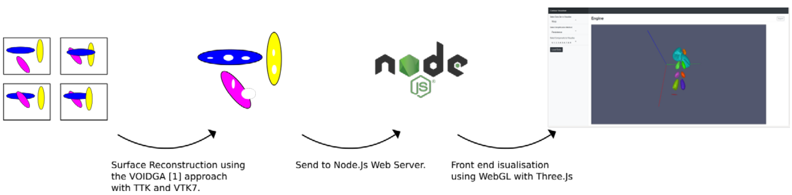

1. “VOIDGA: A View-Approximation Oriented Image Database Generation Approach”, Lukasczyk 2018

UNIVERSITY OF LEEDS

1

Visualizing a Laser Simulation

Multiple isosurfaces (Cluttered)

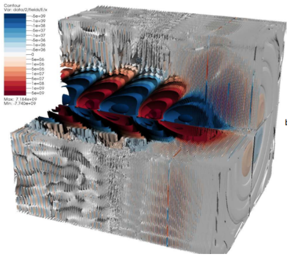

Top ten individual contours (Clear)

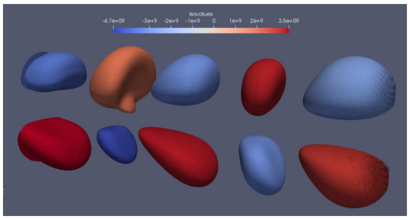

WarpX Simulation:
Data Type = Scalar Field
Data Size = 7GB
Data Dimensions = 6791 x 371 x 371

Contour Tree analysis:
1. Compute the Contour Tree
2. Simplify the Contour Tree
3. Extract contours using the Contour Tree

Problems with multiple Isosurfaces:
- Manual selection of isovalues.
- Occlusion of connected components.
- Noise and unwanted features.

Advantages of contour tree analysis
- Limited user interaction.
- Automatic removal of noise.
- Supports multiple importance metrics.

UNIVERSITY OF LEEDS

Performance & Evaluation

Dataset	Dimensions	Contour Tree Supernodes	Compute Tree seconds	Hypersweep seconds	Branch Decomp seconds	Ratio HS / CT	Ratio BD / CT
WarpX_E_x	6791x371x371	288,807	317.191	0.005	0.055	0.01%	0.01%
Spathorhynchus	1024x1024x750	44,554,912	330.926	0.459	7.299	0.13%	2.20%
Kingsnake	1024x1024x795	55,778,125	268.833	0.589	8.887	0.21%	3.30%
Pawpawsaurus	958x646x1088	89,117,386	352.491	0.979	13.841	0.27%	3.92%

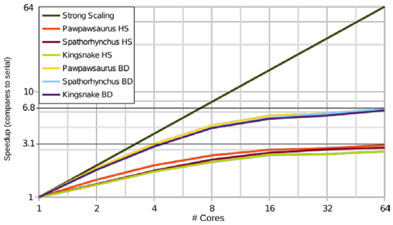

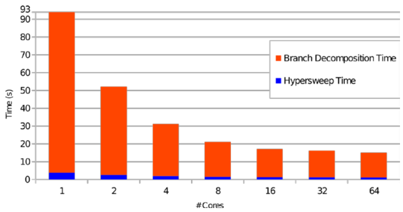

1

UNIVERSITY OF LEEDS

Acknowledgments

This research was supported by:

- **Exascale Computing Project** (17-SC-20-SC), a collaborative effort of the U.S. Department of Energy Office of Science and the National Nuclear Security Administration under Contract No. DE-AC02-05CH11231 (Lawrence Berkeley National Laboratory), Award Number 14-017566 (Los Alamos National Laboratory), and Subcontract 7452335 (University of Leeds).
- School of Computing at the **University of Leeds** (Scholarship to P. Hristov)
- Resources of the **National Energy Research Scientific Computing Center** (NERSC), a U.S. Department of Energy Office of Science User Facility operated under Contract No. DE-AC02-05CH11231.

We thank Jean-Luc Vay and Maxence Thevenet for making the WarpX dataset available.

UNIVERSITY OF LEEDS

Design of Multimodal Test Problems in Multiobjective Optimization Using Fiber Topology

Reiya Hagiwara (Kyushu U.)
Naoki Hamada (KLab Inc., RIKEN AIP)
Takahiro Yamamoto (Tokyo Gakugei U.)
Daisuke Sakurai (Kyushu U.)

Creating a World of Excitement

Contents

- Multiobjective optimization
  - Problem definition
  - Multimodality of test problems
- Relation to fiber topology
  - Local Pareto set and singular set
  - Singular fiber of locally Pareto-optimal value
- Design of multimodal test problems
  - Fiber of local Pareto set of $f\colon \mathbb{R}^3 \to \mathbb{R}^2$
  - Triangulation

Multiobjective optimization

A problem of optimizing multiple functions

E.g. minimize
$$f_1(x_1, x_2) = (x_1 + 1)^2 + (x_2 + 1)^2$$
$$f_2(x_1, x_2) = (x_1 - 1)^2 + (x_2 - 1)^2$$

subject to $-2 \le x_i \le 2 \ \ (i = 1,2)$

Goal: Find the Pareto set / Pareto front

[Definition] A point x is *Pareto optimal* if there exists no point y such that:

- $f_i(y) \le f_i(x)$ for all i,
- $f_j(y) < f_j(x)$ for some j.

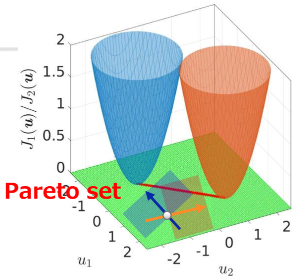

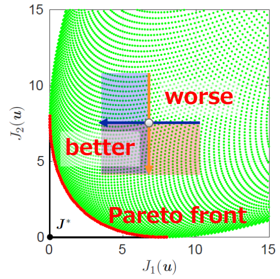

Applications

- Product design
  - Airplane
  - Wind power turbine
- Machine learning / AI
  - Training / hyper-parameter tuning of ML models
  - Game AI
- Planning / Operations
  - Water distribution
  - Assembly line
- Software
  - modeFRONTIER
  - Optimus
  - iSight
  - and more

[MONOist 2014]

[EC-Competition 2019]

Practical problems are “black-box”

- Practical problems involve simulation/experiments
  - Function values are computed by CFD, multi-agent simulation, physical experiments, etc.
  - Closed form expression of functions is unknown
  - Function values at a specified point is available
- Evolutionary multiobjective optimization (EMO)
  - Derivative-free, monte-carlo search
  - Approximate PS/PF with finite points

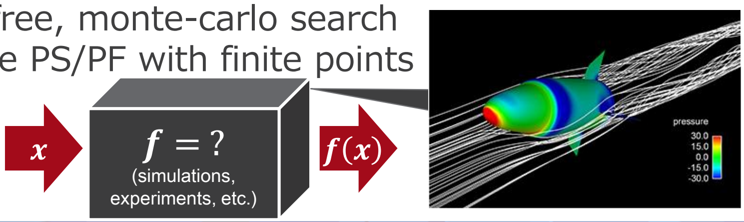

How EMO works

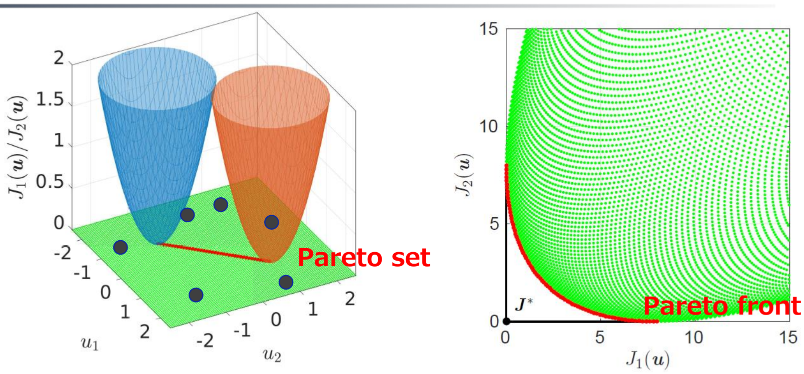

1. Generate random points

For more details, see
[Zhou+ 2011] Multiobjective evolutionary algorithms: A survey of the state of the art , Swarm and Evolutionary Computation 1(1), pp. 32-49.

How EMO works

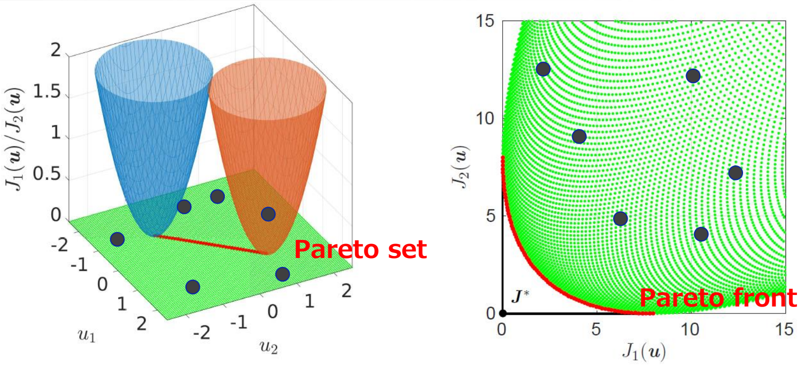

2. Evaluate points

For more details, see
[Zhou+ 2011] Multiobjective evolutionary algorithms: A survey of the state of the art , Swarm and Evolutionary Computation 1(1), pp. 32-49.

How EMO works

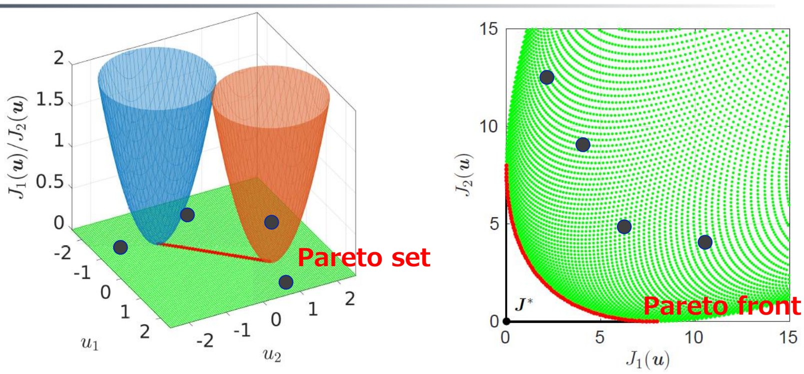

3. Remove “bad” points

For more details, see
[Zhou+ 2011] Multiobjective evolutionary algorithms: A survey of the state of the art , Swarm and Evolutionary Computation 1(1), pp. 32-49.

How EMO works

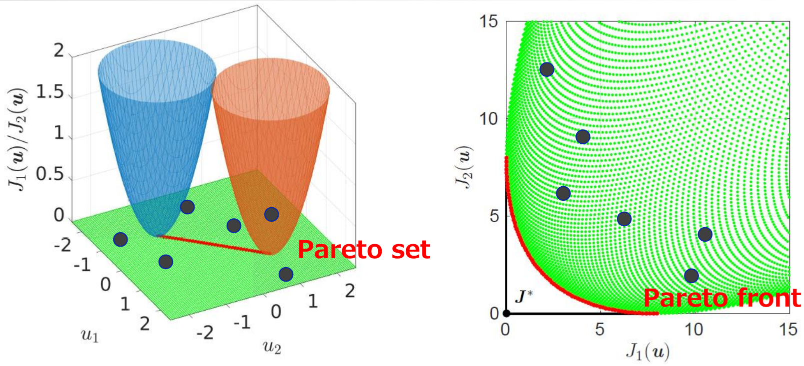

4. Generate points around the current ones

For more details, see
[Zhou+ 2011] Multiobjective evolutionary algorithms: A survey of the state of the art , Swarm and Evolutionary Computation 1(1), pp. 32-49.

How EMO works

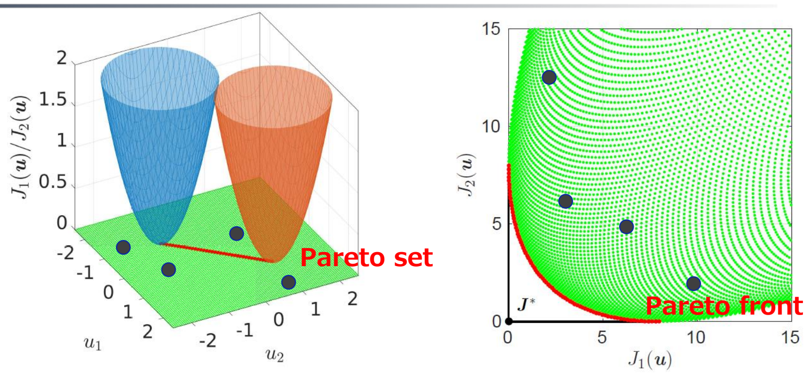

5. Remove “bad” points

For more details, see
[Zhou+ 2011] Multiobjective evolutionary algorithms: A survey of the state of the art , Swarm and Evolutionary Computation 1(1), pp. 32-49.

How EMO works

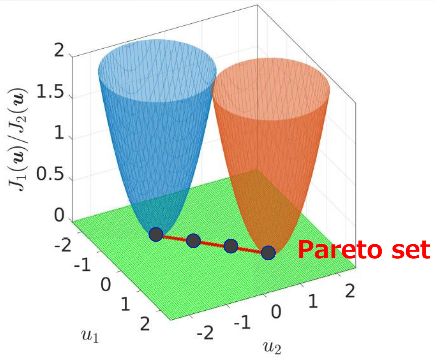

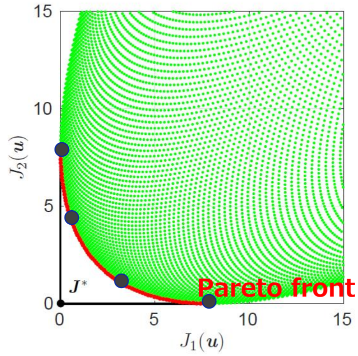

Repeat the steps to find a good approximation

For more details, see
[Zhou+ 2011] Multiobjective evolutionary algorithms: A survey of the state of the art , Swarm and Evolutionary Computation 1(1), pp. 32-49.

Performance comparison of EMO

- Practical problems
  - Real but publicly unavailable
  - Diverse use-cases, no “standard” problem
  - Slow computation (hours ~ days)

    ➡ Hard to use for performance comparison

- Test problems
  - Artificial but publicly available
  - Known features, de facto standard problems
  - Fast computation (seconds ~ minutes)

    ➡ Easy to use for performance comparison

Test problems: History

- **1990~1999**: No standard problem
  - Researchers made their own test problems
- **Early 2000s**: ZDT [Zitzler+ 2000]
  - de facto standard of 2-objective test problems
- **Late 2000s**: DTLZ [Deb+ 2001], WFG [Huband+ 2006]
  - *n*-objective extensions of ZDT
- **2010s**: Inverted-DTLZ [Jain+ 2013], Minus-WFG [Ishibuchi+ 2017]
  - EMOs that have good performance on DTLZ/WFG are bad on Inverted-DTLZ/Minus-WFG
  - Are standard test problems "real"?

How test problems are made: DTLZ

- Split variables

$x = (y_1, \dots, y_{M-1}, z_1, \dots, z_k)$

position vars. **distance vars.**

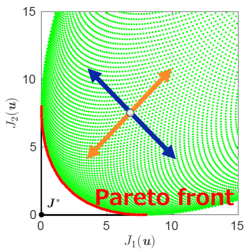

- Compose functions

Polynomials, sin/cos, etc.

TABLE VI

SEVEN OF THE NINE DTLZ MANY OBJECTIVE PROBLEMS. ALL OBJECTIVES ARE TO BE MINIMIZED

Name	Problem	Parameter Domains
DTLZ1	$f_1 = (1+g)0.5\prod_{i=1}^{M-1} y_i$ $f_{m=2:M-1} = (1+g)0.5\left(\prod_{i=1}^{M-m} y_i\right)(1-y_{M-m+1})$ $f_M = (1+g)0.5(1-y_1)$ $g = 100\left[k+\sum_{i=1}^{k}\left((z_i-0.5)^2-\cos(20\pi(z_i-0.5))\right)\right]$	[0, 1]
DTLZ2	$f_1 = (1+g)\prod_{i=1}^{M-1}\cos(y_i\pi/2)$ $f_{m=2:M-1} = (1+g)\left(\prod_{i=1}^{M-m}\cos(y_i\pi/2)\right)\sin(y_{M-m+1}\pi/2)$ $f_M = (1+g)\sin(y_1\pi/2)$ $g = \sum_{i=1}^{k}(z_i-0.5)^2$	[0, 1]
DTLZ3	As DTLZ2, except the equation for g is replaced by the one from DTLZ1.	[0, 1]
DTLZ4	As DTLZ2, except all $y_i \in y$ are replaced by y_i^{α}, where $\alpha > 0$.	[0, 1]
DTLZ5	As DTLZ2, except all $y_2, \dots, y_{M-1} \in \mathbf{y}$ are replaced by $\frac{1+2gy_i}{2(1+g)}$.	[0, 1]
DTLZ6	As DTLZ5, except the equation for g is replaced by $g = \sum_{i=1}^{k} z_i^{0.1}$.	[0, 1]
DTLZ7	$f_{m=1:M-1} = y_m$ $f_M = (1+g)\left(M-\sum_{i=1}^{M-1}\left[\frac{f_i}{1+g}(1+\sin(3\pi f_i))\right]\right)$ $g = 1+9\sum_{i=1}^{k} z_i/k$	[0, 1]

How test problems are characterized

- Several features / recommendations [Huband+ 2006]
  - They are described in natural language
  - No mathematical definition agreed

Name	Objective	R3: # Parameters	F2: Separability	F5: Modality	R1: No Extremal	R2: No Medial	R5: Diss. Domains	R6: Diss. Ranges	R7: Optima Known	F1: Geometry	F3: Bias	F4a: Pareto Many-to-one	F4b: Flat Regions
DTLZ1	$f_{1:M}$	✓*	S*	M	✓	×	×	×	✓	linear	−	+	−
DTLZ2*	$f_{1:M}$	✓*	S*	U	✓	×	×	×	✓	concave	−	+	−
DTLZ3	$f_{1:M}$	✓*	S*	M	✓	×	×	×	✓	concave	−	+	−
DTLZ4	$f_{1:M}$	✓*	S*	U	✓	×	×	×	✓	concave	+	+	−
DTLZ5*	$f_{1:M}$	✓*	?	U	?	?	×	?	×	?	−	+	−
DTLZ6*	$f_{1:M}$	✓*	?	U	?	?	×	?	×	?	+	+	−
DTLZ7	$f_{1:M-1}$	1	NA	U	×	✓	×	×*	✓	disconnected*	−	−	−
	f_M	✓	S	M									

Modality: three definitions

- Definition by local Pareto optima [folklore]
  - A problem is *multimodal* if it has a local Pareto optimum that is not globally Pareto optimal.
- Definition by component modality [Huband+ 2006]
  - A problem is *multimodal* if an objective function has multiple local optima.
- Definition by local Pareto set [Kerschke+ 2016]
  - A problem is *multimodal* if its local Pareto set consists of multiple connected components.

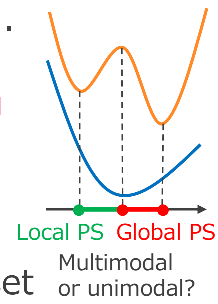

Research questions

- What is a good definition of multimodal problems?
  - Is it defined in terms of fiber topology?
- How to design multimodal test problems?
  - Can we make “flexible” multimodal problems?

Relation to singularity theory

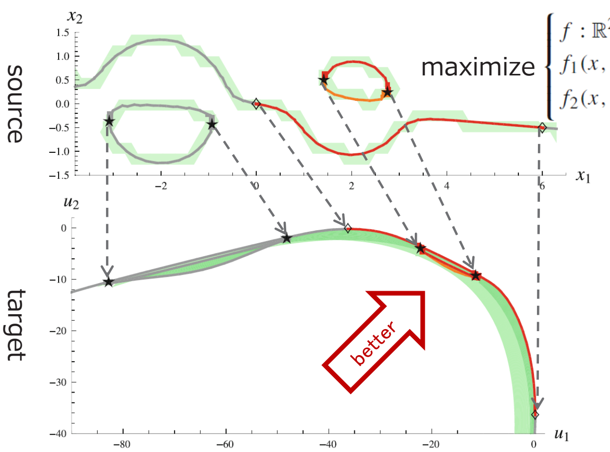

Fig. 1 *Upper panel* Singular set Σ (*gray*, *orange* and *red curves*), critical set θ (*orange* and *red*) and stable critical set θ_s (*red*) for the function in example 1. *Lower panel* Image of the function f with the images of the relevant sets Σ, θ and θ_s highlighted. (Color figure online)

maximize
$$\begin{cases} f : \mathbb{R}^2 \longrightarrow \mathbb{R}^2, \\ f_1(x, y) := -(x-6)^2 - (y+0.5)^2, \\ f_2(x, y) := -x^2 - y^2 - 4\left(e^{-(x+2)^2-y^2} + e^{-(x-2)^2-y^2}\right). \end{cases}$$

If source dim. ≥ target dim.

Singular set
⊃
Pareto critical set
⊃
Local Pareto set
⊃
Pareto set

Local Pareto sets of $f\colon \mathbb{R}^2 \to \mathbb{R}^2$

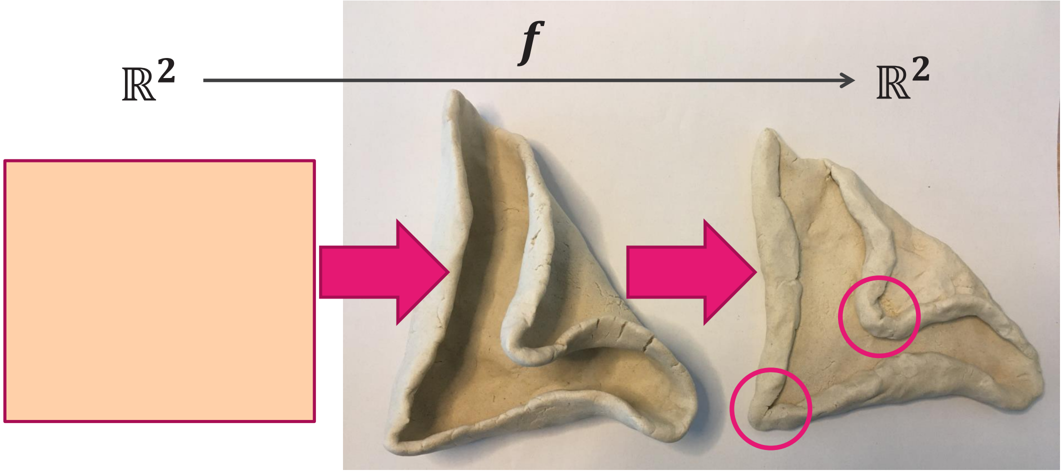

Conclusions

- Fiber topology for multimodal test problems
  - For $\mathbb{R}^3 \to \mathbb{R}^2$, the problem enables us to control
    - The number of modes
    - The location of each mode
    - The shape of each mode
- Future work
  - Benchmarking of EMO methods
  - High-dimensional extension

Practical problems: Few disclosed cases

- Most of them are hidden
- Few problems are disclosed in competitions
  - BBComp
    - Problems are open
    - Solutions are closed
  - EC-Comp
    - Problems are open
    - Solutions are open

EMO'2017 Real-World Problems

The EMO'2017 track (BBComp2017EMO) consists of 10 challenging real-world problems from various domains, listed below. We thank Michael Emmerich for co-chairing this track. The deadline for the track is at midnight UCT on March 14/15, 2017.

problem index	problem name	dimensions	number of objectives	budget
0	welded beam	4	2	100
1	kernel ridge regression	5	2	100
2	brake	4	2	100
3	facility placement	20	2	1000
4	hydro-dynamics	6	2	1000
5	heat exchanger	16	2	500
6	neural network controller	24	2	2000
7	optical filter	11	2	200
8	area under curve	10	2	500
9	vibrating platform	5	2	200

The problem names reflect the underlying problems without giving any details. Beyond the provided problem names, no further information on the problems or their encoding will be provided before the end of the EMO'2017 competition, in order to maintain the black-box character of the competition. We plan to publish the problems after the deadline.

Eco-efficient Flight Trajectory Exploration by Using the Chemistry-climate Model EMAC

Hiroshi Yamashita and Bastian Kern
Institute of Atmospheric Physics, German Aerospace Center (DLR)

DLR

DLR **Deutsches Zentrum für Luft- und Raumfahrt**
German Aerospace Center

DLR at a glance

- Research institution
  - Space Administration
    - Project Management Agency

DLR

Locations and employees

More than 9000 employees work in 54 institutes and facilities at 30 sites across Germany.

International offices in Brussels, Paris, Tokyo and Washington D.C.

DLR

National and international networking

Clients and partners: Governments and ministries, agencies and organisations, industry and business, science and research

DLR

Areas of research:

- Aeronautics
- Space research and technology
- Transport
- Energy
- Security (cross-sectoral area)
- Digitalisation (cross-sectoral area)

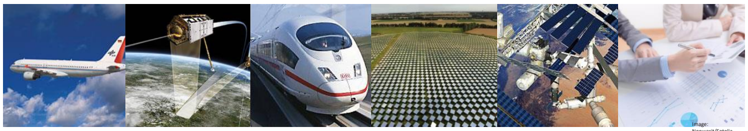

DLR Oberpfaffenhofen

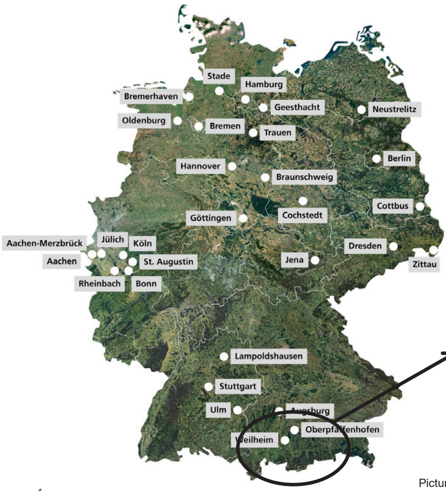

Pictures via Wikimedia Commons: Andreas Steinhoff; Bayreuth2009, CC BY 3.0; Kauk0r, CC BY-SA 3.0; Maximilian Dörrbecker (Chumwa), CC BY-SA 2.5; Ximonic, Simo Räsänen (post-processing) & Tauno Räsänen (photograph), CC BY-SA 3.0

DLR Oberpfaffenhofen

Employees: 1,959
Area: 249,508 m²
Research institutes and facilities:

- Microwaves and Radar Institute
- Institute of Communications and Navigation
- Remote Sensing Technology Institute
- Institute of Atmospheric Physics
- Institute of Robotics and Mechatronics
- Institute of System Dynamics and Control
- German Remote Sensing Data Center
- Flight Experiments Facility
- Complex Plasmas Research Group
- Space Operations and Astronaut Training
- Galileo Control Centre

DLR

The DLR Institute of Atmospheric Physics

Physics and chemistry of the global atmosphere: 0-120 km altitude

Socially relevant issues related to the atmosphere in aviation, space travel, transport and energy

Climate protection, mobility of the future, digitalization & artificial intelligence, energy system transformation

Both basic and application-oriented questions

Broad spectrum of methods

Internationally competitive and in some areas internationally leading

Competent contact for DLR, society, industry and politics

DLR

The institute at a glance

Founded 1.7.1962 (1924)

End of 2019 150 employees (51f, 99m)

thereof ~ 37 PhD students

18 Lectureships/professorships at 9 universities/colleges

Overall budget 2019: 18,8 M€ (~ 2256 M¥)

Basic funding : 13,2 M€

(48% Aerospace, 39% Aviation, 11% Traffic, 2% Energy)

Third-party funds : 5,6 M€ (ESA, EU/ERC, BMBF, BMWi, DFG, HGF, Airbus,…)

DLR

Organization

Institute of Atmospheric Physics
Prof. Markus Rapp
Director

Logistics
Sonja Koch
Stefanie Zähnle
Controlling

Quality Management
Dr. Arthur Schady

Earth System Modelling
Prof. Robert Sausen a)

- **YIG MACClim**
  J.-Prof. Hella Garny

ESM – Evaluation and Analysis
Prof. Veronika Eyring

Atmospheric Trace Species
Dr. Anke Roiger

Cloud Physics
Prof. Christiane Voigt

- **Passive Cloud-Remote Sensing**
  Dr. Luca Bugliaro

Transport Meteorology
Dr. Thomas Gerz

Lidar
Dr. Andreas Fix

- **Lidar/Radar-Synergy**
  Dr. Silke Groß

a) New appointment as of 01.07.2021; W2 appointment procedure with LMU ongoing

close cooperation with LMU LUDWIG-MAXIMILIANS-UNIVERSITÄT MÜNCHEN

DLR

(Numerical) Modelling in a nutshell

- There is no second Earth (to experiment with)

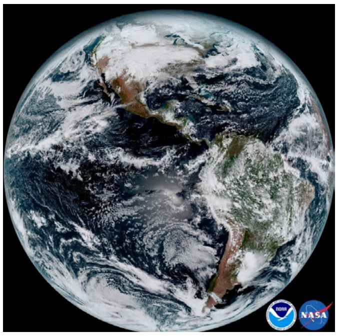

NOAA/NASA
https://www.nasa.gov/image-feature/new-weather-satellite-sends-first-images-of-earth

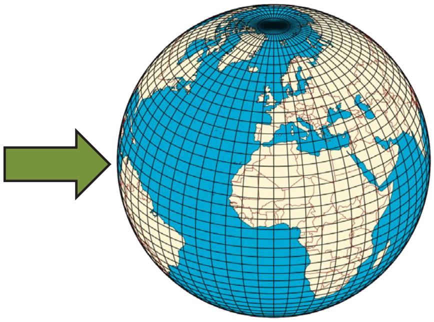

Wikimedia, user Hellerick
https://commons.wikimedia.org/wiki/File:Division_of_the_Earth_into_Gauss-Krueger_zones_-_Globe.svg

DLR

(Numerical) Modelling in a nutshell

- There is no second Earth (to experiment with)
- A mathematical model
  - → based on physical equations
  - → coupled system of (non-linear) partial differential equations
  - → solved numerically on a “supercomputer”

https://www.dkrz.de/about/media/galerie/Media-DKRZ/hlre-3

DLR

(Numerical) Modelling in a nutshell

- There is no second Earth (to experiment with)
- A mathematical model
  - → based on physical equations
  - → coupled system of (non-linear) partial differential equations
  - → solved numerically on a “supercomputer”

- Climate projection (vs. weather forecast)
  - no forecasts, but climate projections → statistical analyses
  - boundary value problem (vs. initial value problem)
  - model produces realistic weather systems from internal variability

Modular Earth Submodel System (MESSy)

https://www.messy-interface.org/

> 20 partner institutes

Framework to couple scientific codes to numerical weather prediction and climate models

EMAC = **E**CHAM/**M**ESSy **A**tmospheric **C**hemistry

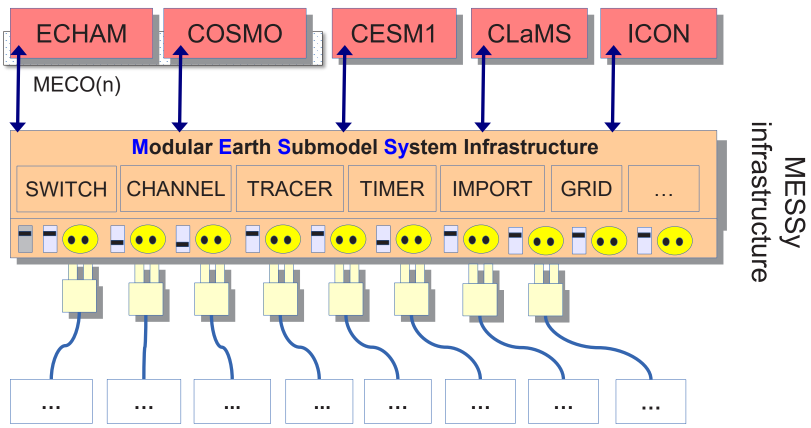

Climate projections with EMAC

- Model simulations with 2 PByte output
- Contribution to Chemistry Climate Initiative (CCMI)
- Data for WMO Ozone Assessment and Intergovernmental Panel on Climate Change (IPCC)

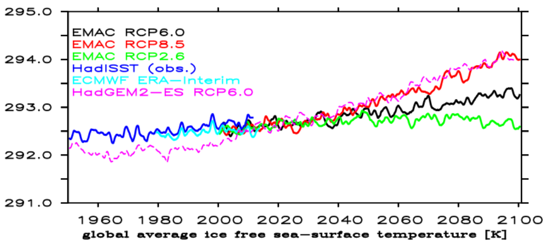

Total ozone column (DU), Antarctic, October

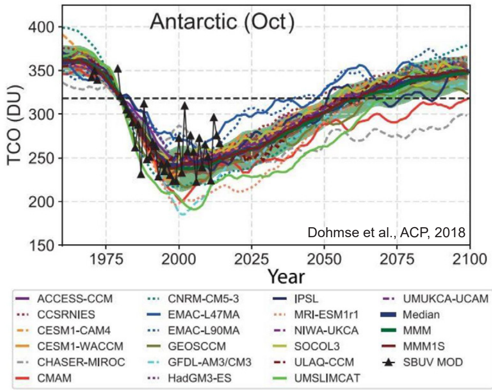

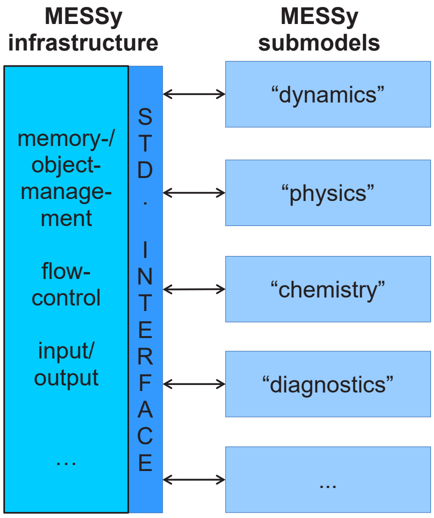

"communication" between individual components through mutual access of distributed objects via standard interfaces

expandability without intervention in other components

- scalable development
- coexistence of alternatives

→ **"community"-ansatz**

2nd part

Application study

Contents

- Aviation and climate impact
- Climate-optimized routing
- Research objectives and methodologies
- EMAC/AirTraf model components
- 1-day air traffic simulations over the North Atlantic with different aircraft routing options
- Multi-objective optimization in EMAC/AirTraf
- Summary – research topics for further collaborations

Growth of air transport

- Strong growth in air traffic: +5 %/yr (1945 - 2019)
- World passenger traffic collapsed due to COVID-19 Pandemic, but it is recovering

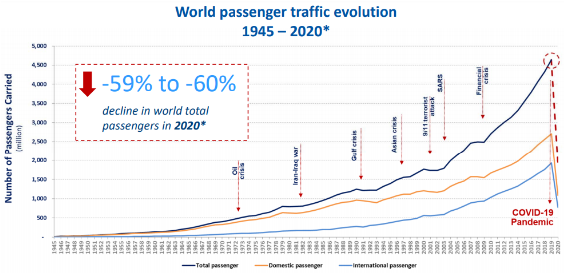

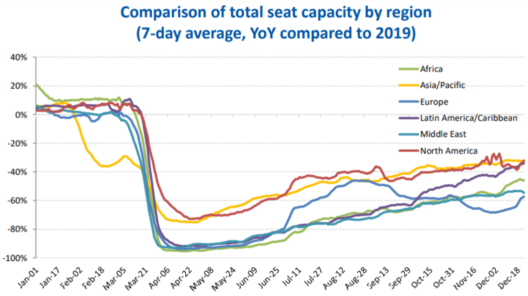

ICAO 2020

DLR

Aviation emissions and climate change

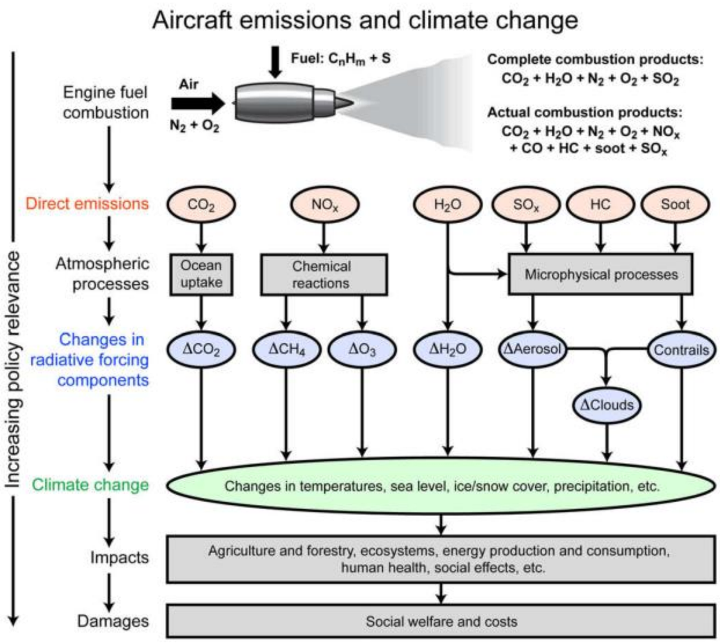

Lee et al. 2009

DLR

Aviation and radiative forcing for 2005

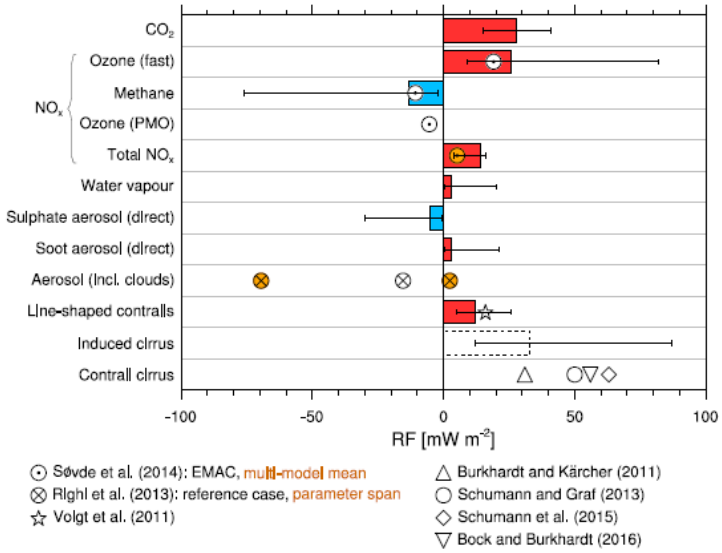

Grewe et al. 2017

Impact of aviation on global surface temperatures

- Air traffic contributes around 5 % to anthropogenic warming

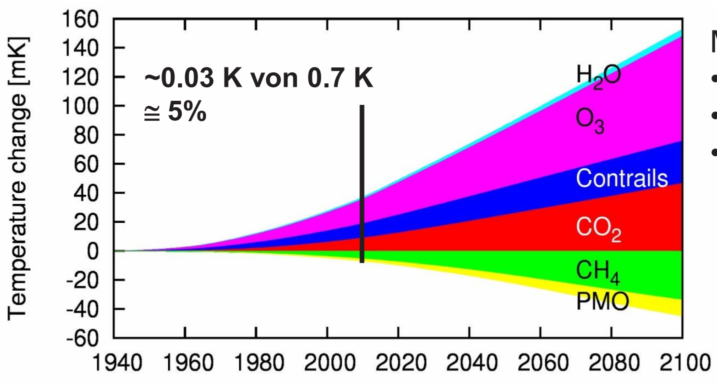

Main contributions from:

- CO_2
- Contrails
- NO_x (O_3 and CH_4)

PMO=„Primary mode ozone“
Results from less $CH_4 \Rightarrow$ less $HO_2 \Rightarrow$ less O_3 production

Grewe et al. 2016

Climate-optimized routing

- "Climate cost function (CCF) identifies climate sensitive regions for emissions (CO_2, H_2O, ozone, Methane, contrails) and estimates climate impacts
- Climate-optimal route was calculated by air traffic simulator SAAM by Eurocontrol:
  - −19 % less climate impact
  - 1 % longer flight time
  - 14 % more fuel
  - 22 % more NO_x
  - 10 % more costs

Example of route options for one flight from Washington to Vienna (AGWP20)

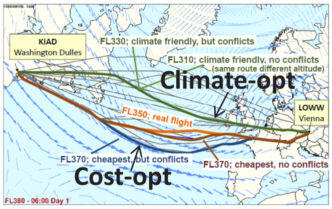

Frömming, et al. 2013
Grewe, et al. 2014, 2017
Matthes, et al. 2012,2017

DLR

Research objectives

- To investigate an eco-efficient aircraft routing strategy that reduces the climate impact of global air traffic over the next few decades
- To estimate its mitigation gain for different aircraft routing strategies

Methodologies

- **Chemistry-climate model EMAC (ECHAM5/MESSy 2.54)** Roeckner et al., 2006; Jöckel 2010, 2016
- **Submodel AirTraf 2.0** Yamashita, Kern et al. 2020
  - 9 routing strategies (called options)
  - Trajectory optimization (3D)
  - Geographic location, altitude, time of released non-CO_2 emissions/contrails are considered
  - Simplifications:
    - Only cruise flight phase
    - No potential conflicts of flight trajectories
    - No operational constraints from ATC

Aircraft routing options

0 - **Great circle**
1 - **Flight time**
2 - **Fuel use**
3 - **NO_x emission**
4 - **H_2O emission**
5 - **Contrail formations**
6 - **Simple operating cost**
7 - **Cash operating cost**
8 - **Climate impact**

EMAC/AirTraf model components

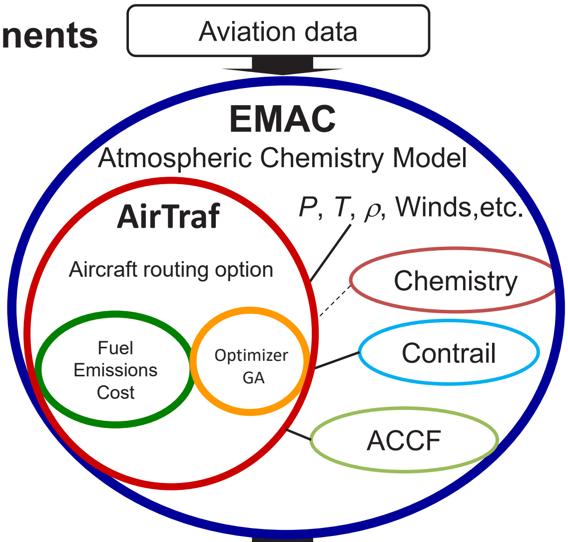

Base model

ECHAM5/MESSy 2.54 (EMAC)

Roeckner et al., 2006, Jöckel 2010, 2016

Submodel AirTraf 2.0

Aviation data

- ICAO engine performance data
- Aircraft data (BADA 3.9)
- Flight plan, fuel price, etc.

Fuel/emissions calc.

- Total energy model
- DLR fuel flow correlation method

Deidewig 1996, Schaefer 2012

Optimizer

- Genetic algorithms (ARMOGA1.2.0)

Sasaki, 2009

Coupled submodels

- CONTRAIL 1.0
- ACCF 1.0

Van Manen, 2017,2019; Yin, 2018,2020

- Optimized flight trajectories
- Flight performance measures:
  - Flight distance, flight time, fuel use, NO_x emission, H_2O emission, contrail distance, operation cost, climate impacts (ATR20s)
- Radiative forcing (surface temperature change)

Flight trajectory optimization

- A trajectory (candidate) is created by B-spline curve with 11 design variables: **6 (geographical location), 5 (altitude)**
- Waypoints are automatically generated
- GA evaluates single objective function and finds out one optimal trajectory to minimize objective function value

Objective function

$$\text{Minimize } f \quad \text{Subject to } x_j^l \le x_j \le x_j^u,\ j = 1, 2, \cdots, n_{dv}$$

Yamashita et al. 2016

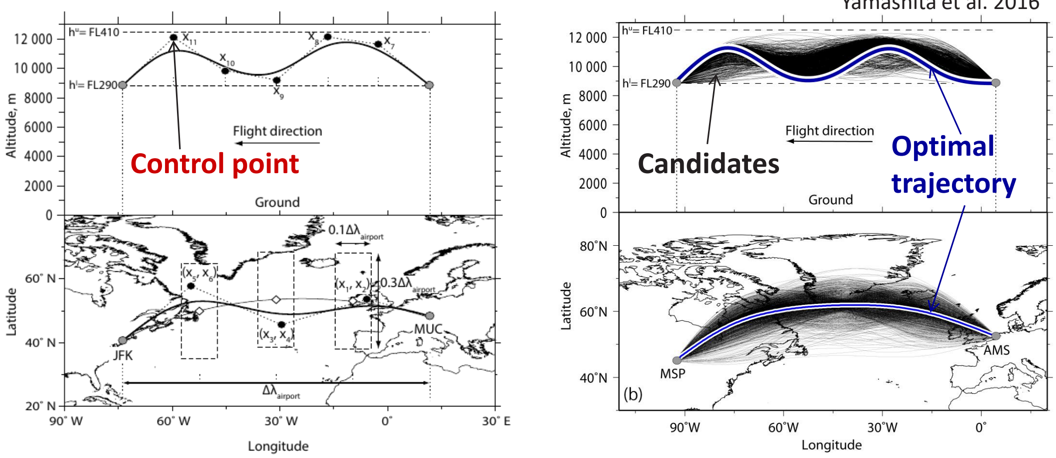

Formulations of objective functions

- **Cost option**
  - Min. Cash Operating Cost (international flights [USD]) Liebeck, 1995

$$f = COC = C_{\text{flightcrew}} + C_{\text{cabincrew}} + C_{\text{landing}} + C_{\text{navigation}} + C_{\text{fuel}} + C_{\text{airframe}} + C_{\text{engine}}$$

- **Climate option**
  - Submodel ACCF 1.0
  - Min. climate impact over 20 yrs [K] estimated by algorithmic Climate Change Functions aCCFs Van Manen, 2017,2019; Yin, 2018,2020

$$\begin{aligned}
\text{ATR20}_{\text{O}_3,i} &= \text{aCCF}_{\text{O}_3,i} \times \text{NO}_{x,i} \times 10^{-3},\\
\text{ATR20}_{\text{CH}_4,i} &= \text{aCCF}_{\text{CH}_4,i} \times \text{NO}_{x,i} \times 10^{-3},\\
\text{ATR20}_{\text{H}_2\text{O},i} &= \text{aCCF}_{\text{H}_2\text{O},i} \times \text{FUEL}_i,\\
\text{ATR20}_{\text{CO}_2,i} &= \text{aCCF}_{\text{CO}_2} \times \text{FUEL}_i,\\
\text{ATR20}_{\text{contrail},i} &= \text{aCCF}_{\text{contrail},i} \times \text{PCC}_{\text{dist},i},
\end{aligned}$$

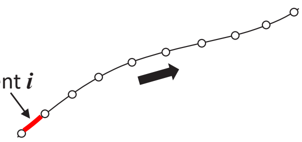

$$\text{ATR20}_{\text{total},i} = \text{ATR20}_{\text{O}_3,i} + \text{ATR20}_{\text{CH}_4,i} + \text{ATR20}_{\text{H}_2\text{O},i} + \text{ATR20}_{\text{CO}_2,i} + \text{ATR20}_{\text{contrail},i},$$

$$f = \sum_{i=1}^{n_{\text{wp}}-1} \text{ATR20}_{\text{total},i},$$

1-day air traffic simulations over the North Atlantic

Routing options	Great circle	Cost/Climate/Others options
ECHAM5 Resolution	T42/L31ECMWF (2.8° × 2.8°)	
Duration / Time step	Dec.01.2015 - Dec.02.2015 / 12 min	
Waypoints	101	
Flight altitude change	Fixed FL350	FL290 - FL410
Flight plan	103 Transatlantic flights by REACT4C Project (Eastbound 52/Westbound 51)	
Aircraft / Engine type	A330-301 / CF6-80-E1-A2 (2GE051)	
EIH_2O [g(H_2O)/kg(fuel)]	1,230 (IPCC 1999)	
Load factor	0.62 (ICAO 2009)	
Fuel price [USD/USG]	1.545 (IATA 2017)	
Unit time cost [USD/h]	2710.0 (Boeing 2015)	
Mach number	0.82 (A330-301, Eurocontrol 2011)	
Optimization	–	Min. *f* **(single-objective optimization)**
Design variable	–	11 (Location 6/Altitude 5)
Generation number	–	100
Population size	–	100

Optimized flight trajectories

Dec. 1 2015, 103 North Atlantic flights (A330-301)

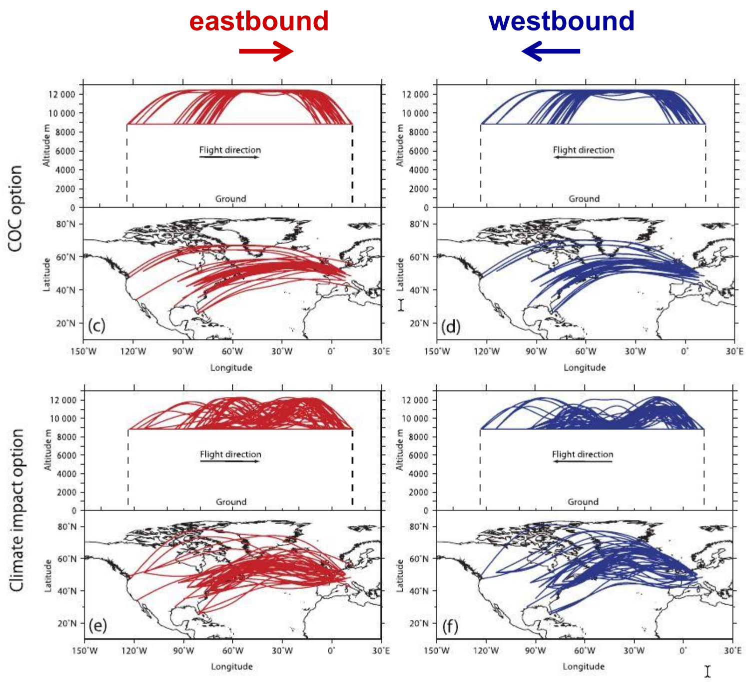

Yamashita, Kern et al. 2020

Distribution maps

Dec. 1 2015, 103 North Atlantic flights (A330-301)

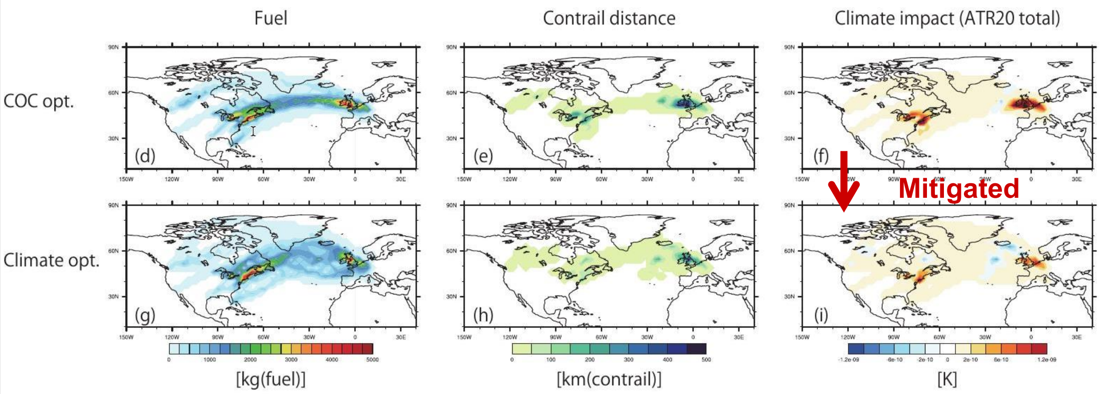

Yamashita, Kern et al. 2020

Flight characteristics

Dec. 1 2015, 103 North Atlantic flights (A330-301)

- Trade-off exists between operational cost and climate impact
- Climate-optimized routing can reduce expected climate impact (ATR20), compared to cost-optimized routing
  - Climate option: –67.9 % ATR20, +9.8 % COC → 0.13 [US Mil$/$10^{-7}$K]

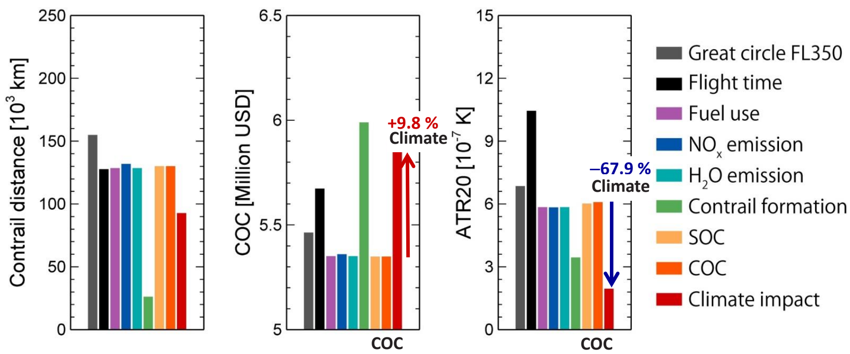

Yamashita, Kern et al. 2020

Multi-objective flight trajectory optimization in AirTraf

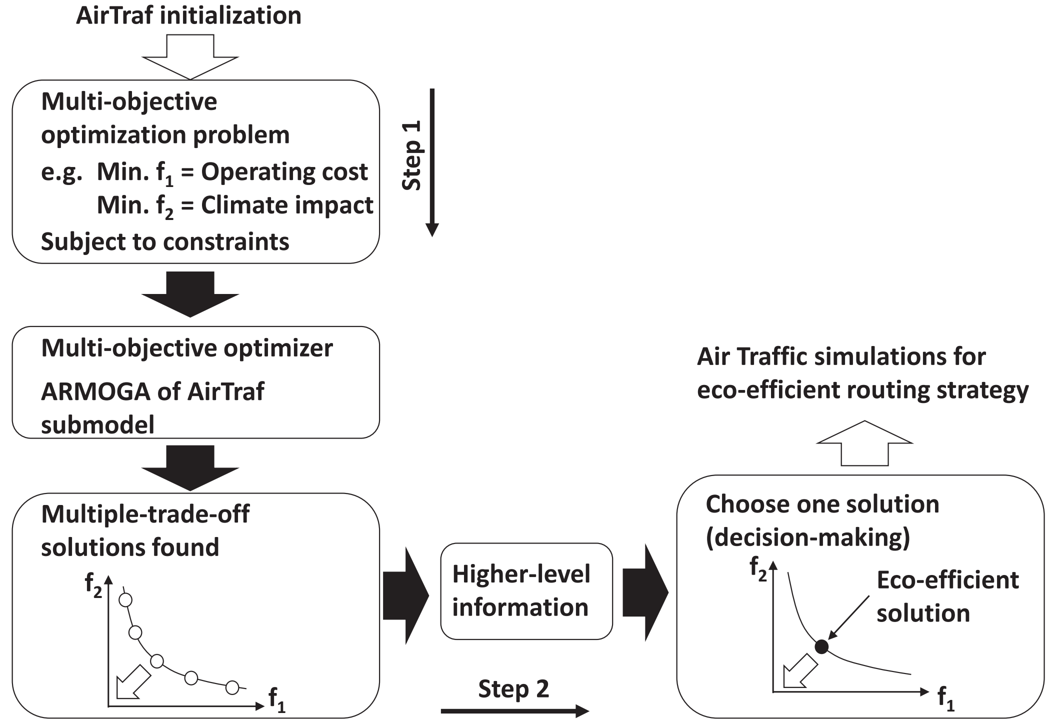

Deb 2001

Benchmark test

Min. f_1 = Flight time [s]
Min. f_2 = Fuel use [kg(fuel)]
Min. f_3 = Climate impact (ATR20) [K]
Flight route: from JFK (New York) to CDG (Paris), flight alt. at FL290 (fixed)
Target day: 01 June 2015
Departure time (local time): from 07:00 to 17:00 (every 2h)

1534 optimal solutions

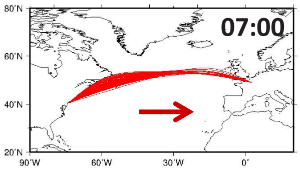

1384 optimal solutions

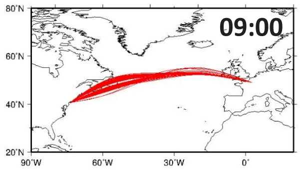

813 optimal solutions

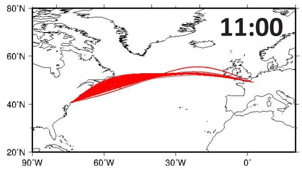

1403 optimal solutions

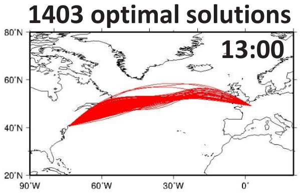

679 optimal solutions

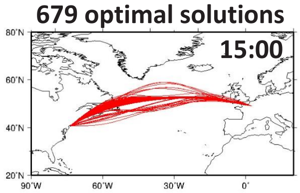

951 optimal solutions

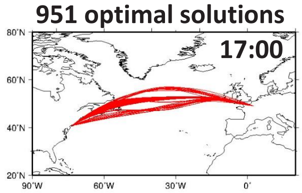

Non-dominated solutions

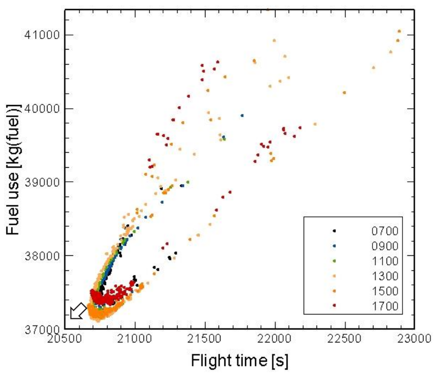

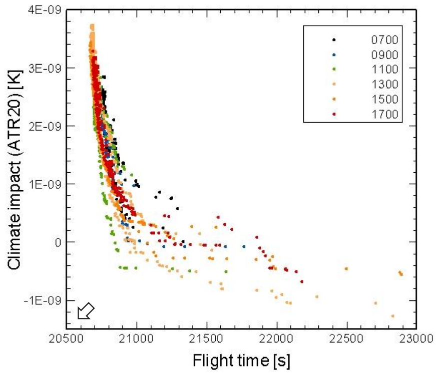

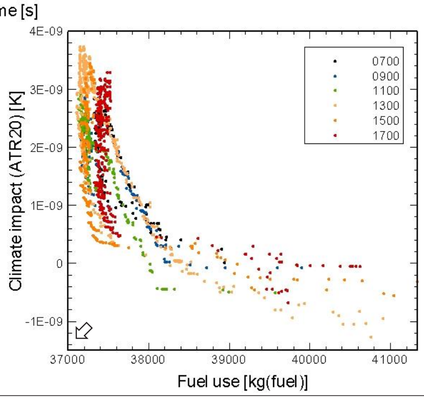

Summary – research topics for further collaborations

1. To detect some unique points of the nondominated solutions and visualize the structure of nondominated fronts

2. To examine how much nondominated fronts vary under different weather conditions

3. To develop a decision-making method in EMAC/AirTraf

Elimination of B_2 singularities

Takahiro YAMAMOTO

Department of Mathematics, Tokyo Gakugei University

8 January, 2021

Fiber Topology Meets Applications

Kyushu University/ ZOOM

§ 0-1 Takahiro YAMAMOTO（山本　卓宏）

INTEREST: To study TOPOLOGY or GEOMETRY of spaces M, in particular manifolds, by using singularity of smooth maps $f\colon M \to \mathbb{R}^k$, ($\dim M \geq k$).

KEY WORDS: Stable maps, Generic maps, Singular Points, Singular Fibers

Favorit formulas: [Kamenosono -**Y**('08)] For a stable map $f\colon \Sigma_g \to S^2$, we have

$$g = N + \frac{c}{2} + (1 + I) - m(f).$$

[Saeki -**Y**('06)] For a stable map $f\colon M \to \mathbb{R}^3$ of a closed oriented 4-mfd, we have

$$\sigma(M) = ||\mathrm{III}^8(f)||.$$

the signature of M

singular fiber

Joint Works with Computer Sci.:

(By O. Saeki, S. Takahashi, D. Sakurai, H. Wu, K. Kikuchi, H. Carr, D. Duke, **Y**)

(1) *Visualizing Multivariate Data Using Singularity Theory*, The Impact of Applications on Mathematics, Proceedings of Forum of Mathematics for Industry 2013, 51–65.

(2) *Interactive Visualization for Singular Fibers of Functions $f\colon \mathbb{R}^3 \to \mathbb{R}^2$*, IEEE TRANSACTIONS ON VISUALIZATION AND COMPUTER GRAPHICS, VOL. 22, NO. 1, 945–954, JANUARY 2016.

! Contributed by classifying singular fibers of stable maps $M^3 \to \mathbb{R}^2$ of cpt 3-mfds with boundary...

(D. Sakurai, **Y**) (3) *Visually Evaluating the Topological Equivalence of Bounded Bivariate Fields*, accepted for publication in the Springer book on Topological Data Analysis following the TopoInVis 2019 workshop.

! Contributed by constructing the theory and calculating example by using "jcnet".

§ 0-2 Introduction

In this talk, mfd.s and maps are smooth of class C^∞ unless otherwise stated.

A smooth stable map, stable map for short is a smooth map s.t. any maps close to the map are equivalent to the map, $f\colon M \to P$ of a cpt mfd M with bdry into a surface P without bdry admits singularities which consists of

folds, cusps, bdry folds, B_2 (and bdry cusps if dim $M \geq 3$).

In this talk, we

- **give** a set of local moves for stable maps $f\colon M \to P$, and
- **study** the question: Given M, a stable map $f\colon M \to \mathbb{R}^2$, can f be deformed to a stable map g s.t. g has **NO** B_2 singularities.

! It is a fundamental problem if generic singularities are eliminated by generic homotopy in singularity theory of smooth maps.

Contents:

How to eliminate B_2 singularities (The case of dim $M = 2$):

Here are pictures of a cup taken from different angles. The picture on the left is taken from an oblique angle, and the object has **TWO** B_2 points. The pictures on the right shows the object viewed from directly above, and the picture in the middle is at in-between angle of the pictures on both sides. In the middle picture, the pair of B_2 points comes in collision, and the object eventually has **NO** B_2 points in the left picture.

§ 1. Preparation and Main-Theorem

Let M: a closed (i.e. compact without boundary) manifold (dim$M \geq$ 2).
For a C^∞ map $f: M \to N$, denote by

$$S(f) = \{p \in M \mid \text{rank}(\partial f_i/\partial x_j)(p) < \min\{\dim M, \dim N\}\}$$

the set of singular points of f, where $f = (f_1, \ldots, f_n)$ denotes local form of f around p.

History of **Elimination of singularities** of C^∞ maps $M \to N$ by generic homotopy, i.e. generic deformation of maps:

Whitney ('44): **Whitney umbrellas** of $f: M^n \to \mathbb{R}^{2n-1}$.
Levine ('66) $n > 2$; **Eliashberg ('72)** $n = 2$: **Cusps** of $f: M^n \to \mathbb{R}^2$.
Cf. **Ando ('85)**: **Morin singularities** of $f: M \to \mathbb{R}^n$.
Saeki ('06): **Definite folds** of $f: M^n \to S^2$, $n \geq 2$

M are closed mfds

!!Today: **B_2s** of $f: M \to \mathbb{R}^2$, where M is a cpt. mfd with bdry.

Let M: a mfd with bdry and P: a mfd without bdry,

$f\colon M \to P$ is **stable**
$\overset{\text{def}}{\Leftrightarrow}$ $\exists N(f) \subset C^\infty(M,P)$: a nbd of f with respect to the Whitney C^∞ topology
s.t.

for any $g \in N(f)$, f and g are equivalent,

where f and g are equivalent if there exist $s \in \mathrm{Diff}(M)$ and $t \in \mathrm{Diff}(P)$ s.t. $t \circ f = g \circ s$.

! Any $s \in \mathrm{Diff}(M)$ preserves ∂M.

Proposition 1.2 ($\dim M = 2$)

M: a cpt surface with bdry, P: a surface without bdry.
$f\colon M \to P$ is **stable** $\overset{\text{iff}}{\Leftrightarrow}$ it is locally one of the following:

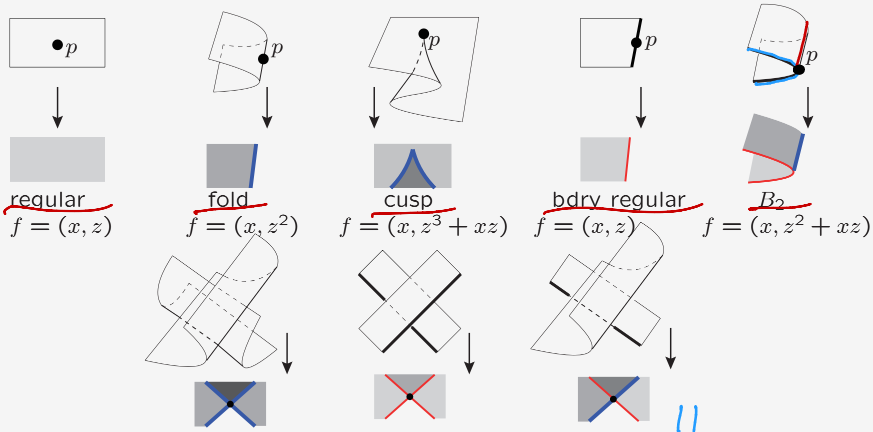

! If a C^∞ map $f\colon M \to \mathbb{R}^2$ is stable, then $f|_\partial$ is also stable.

! $S(f)$ consist of **finite number of circles and arcs**.

Example: stable maps of cpt surf.s with bdry into the plane

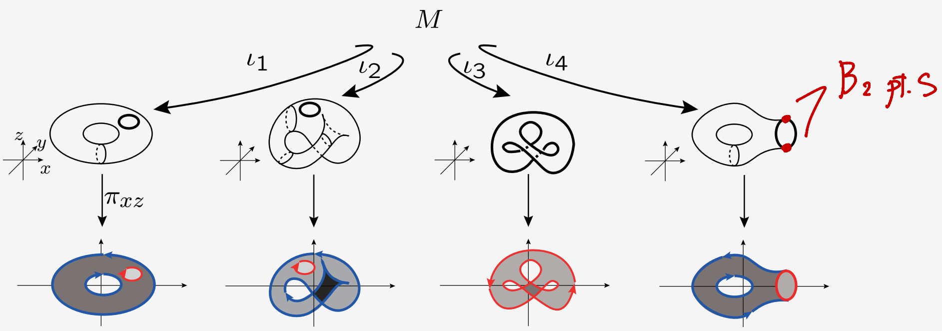

$f_i \colon M \to \mathbb{R}^2$ $(i = 1, 2, 3, 4)$ defined by $f_i = \pi_{xz} \circ \iota_i$ are stable maps of torus with one bdry component. f_1, f_2 and f_3 have **NO** B_2 points. f_3 has **NO** singular point. f_4 has **TWO** B_2 points.

Proposition 1.3 (dim$M = 3$)

M: a cpt mfd with bdry, P: a surface without bdry.

$f \colon M \to P$ is **stable** $\overset{\text{iff}}{\Leftrightarrow}$ ~~locally it is one of the following~~:

(1) $\forall p \in M$, nbds of p in their level sets are one of the items belows:

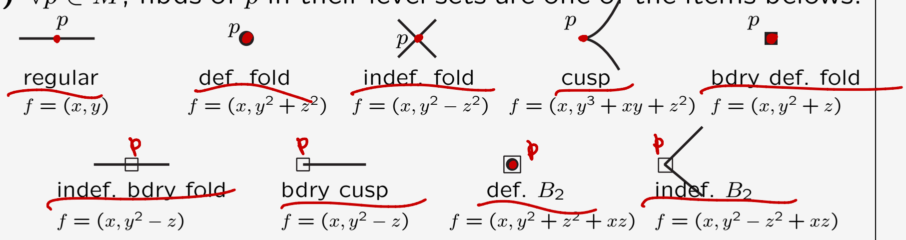

where the black dot, the black square, and the black dot surrounded by a square represent an isolated point; however, we use distinct symbols in order to distinguish their corresponding map germs. The squares represent points on the boundary.

(2) ...

Proposition 1.3 (dim$M = 3$):Conti.

M: a cpt mfd with bdry, P: a surface without bdry.

$f\colon M \to P$ is **stable** $\overset{\text{iff}}{\Leftrightarrow}$ it satisfies the following conditions:

(1) ...

(2) $^{\forall}q \in f(S(f) \cup S(f|_{\partial}))$, nbds of q in $f(S(f) \cup S(f|_{\partial}))$ is one of the items belows:

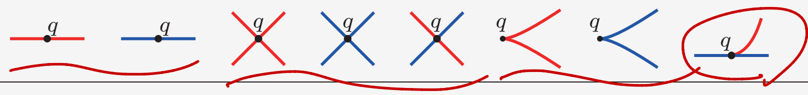

! $S(f)$ and $S(f|_{\partial})$ consist of **finite number of circles and arcs**, and **finite number of circles** respectively.

! If a C^{∞} map $f\colon M \to P$ is stable, then $f|_{\partial}$ is also stable.

! For a regular value $q \in P$, the pre-image $f^{-1}(q)$ consists of finite number of **circles** and **arcs**.

! Stable maps $f\colon M \to P$ of cpt n-mfd.s ($n \geq 4$) with bdry into surf.s without bdry are also characterized as well.

$f\colon X \to Y$: cont. map between topological spaces, $x, x' \in X$

$x \sim x' \overset{\text{def}}{\Leftrightarrow} \exists y \in Y$ s.t. x and x' are in the same conn. comp. of $f^{-1}(y)$

! $\sim$ is an equiv. relation.

Then, the **Reeb space** of f is defined by $W_f := X/\sim$. In particular, if f is a function, then W_f is called the **Reeb graph** of f.

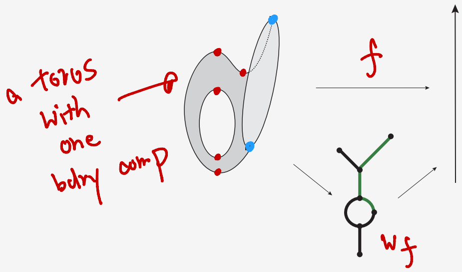

Black and **Green** arcs of W_f correspond to circle pre-images and arc pre-images respectively.

In order to study Reeb spaces of a stable map $f\colon M \to P$ of a 3-mfd with bdry into a surf., we recall the the behaviour of level set near a singular point $p \in S(f) \cup S(f|_\partial)$:

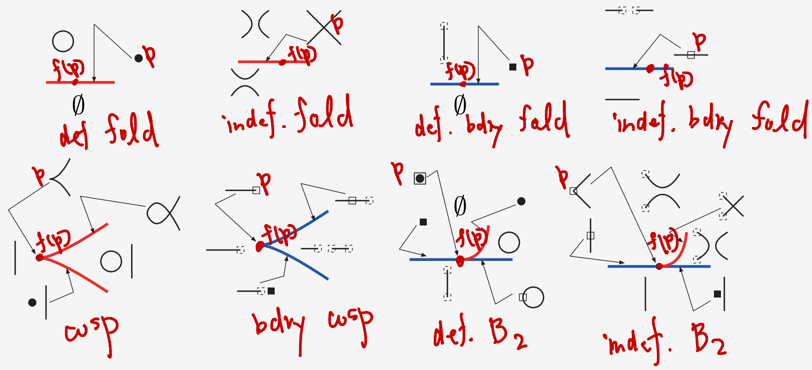

Reeb space W_f of a stable map $f\colon M \to P$ of a 3-mfd with bdry into a surf. is a polyhedron locally characterized by the following manner:

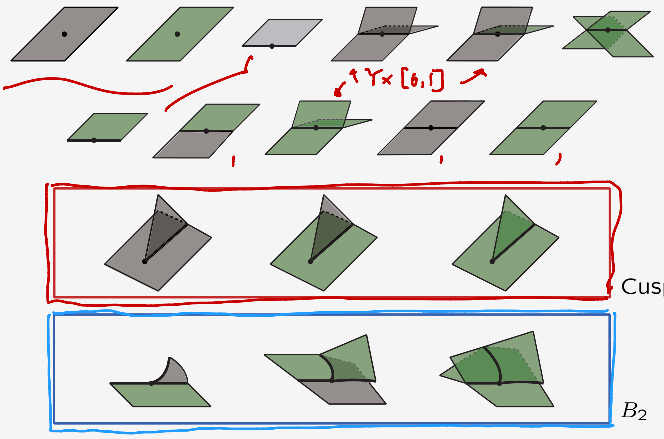

Cusps and bdry cusps

B_2

! Gray regions and Green regions of W_f correspond to circle pre-images and arc pre-images respectively.

! There are 27 other types corresponding to multi-germs of folds and bdry folds.

§ 2 Local moves

Consider a C^∞ homotopy τ as a path $\tau\colon [0,1] \to C^\infty(M, P^2)$, $\tau(t) = \tau_t$.

By using the parametrized transversality theorem, we call a C^∞ homotopy τ a **generic homotopy** if it satisfies the following condition: $\exists t_1, \ldots, t_k \in (0,1)$ such that

(1) $\forall t \in (0,1) \setminus \{t_1, \ldots, t_k\}$, τ_t is a stable map,
(2) $\forall t_i$, $(i = 1, \ldots, k)$, $\exists_1 y_i \in P^2$ and $\exists S_i \subset \tau_{t_i}^{-1}(y)$: a finite set, s.t. $\tau_{t_i}\colon (N, S_i) \to (P^2, y_i)$ is equivalent to one of the germs below:

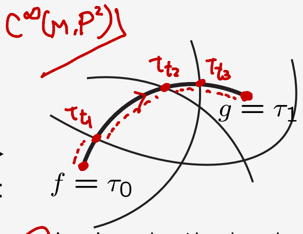

! For $t_{i-1} < t < t_i < t' < t_{i+1}$, the deformation of τ_t into $\tau_{t'}$ is given by the local moves given below.

(mono-germs) dim $M = 2, 3$,

lip $\tau_t = (x, z^3 + z(x^2 - t) \pm y^2)$
beak $\tau_t = (x, z^3 - z(x^2 - t) \pm y^2)$
Swallow-tail $\tau_t = (x, z^4 + tz^2 + xz \pm y^2)$

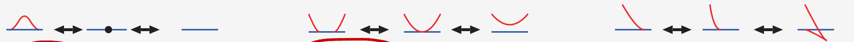

B_2-lip $\tau_t = (x, z^2 + z(x^2 - t) \pm y^2)$
B_2-beak $\tau_t = (x, z^2 - z(x^2 - t) \pm y^2)$
B_3 $\tau_t = (x, z^3 + xz + tz^2 \pm y^2)$

dim $M = 3$

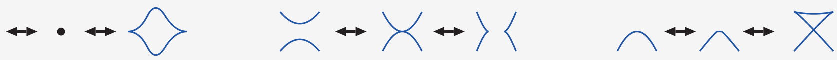

Bdry Lip $\tau_t = (x, z^3 + z(x^2 - t))$
Bdry beak $\tau_t = (x, z^3 + z(x^2 - t))$
Bdry Swallow-tail $\tau_t = (x, z^3 + z(x^2 - t))$

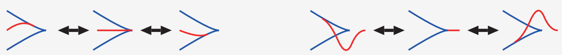

def C_3 $\tau_t = (x, z^3 + z(x^2 - t))$
indef C_3 $\tau_t = (x, z^3 - z(x^2 - t))$

def/indef B_2-lip: $f_t = (x, \pm z^2 + z(x^2 - t) \pm y^2)$

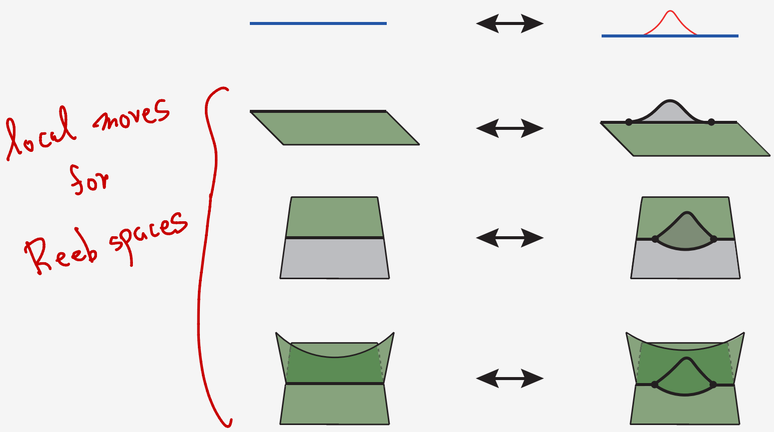

def/indef B_2-beak: $f_t = (x, z^2 - z(x^2 - t) \pm y^2)$

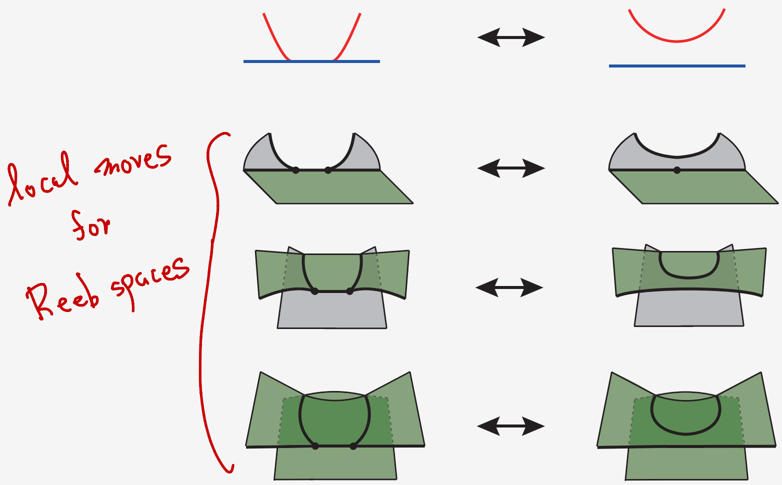

def/indef-B_3: $f_t = (x, \pm z^3 + xz + tz^2)$

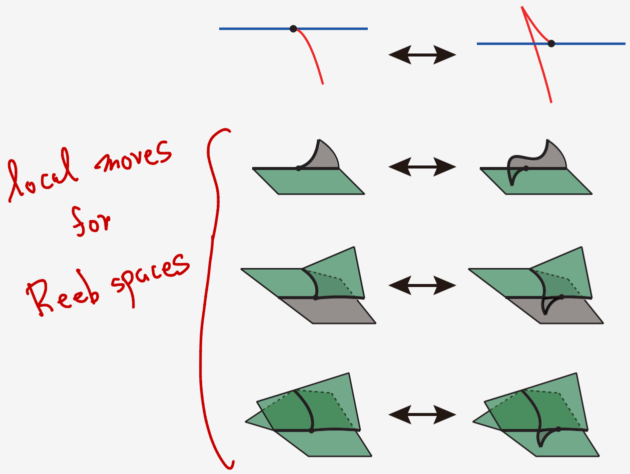

def-C_3: $f_t = (x, yz + y^3 + xy + tz)$

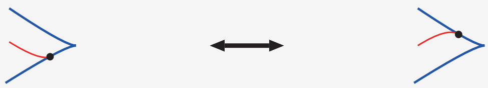

indef-C_3: $f_t = (x, yz - y^3 + xy + tz)$

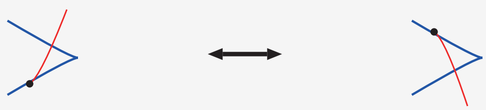

(multi-germs): $\tau_t(S(\tau_t) \cup S(\tau_t|_\partial))$

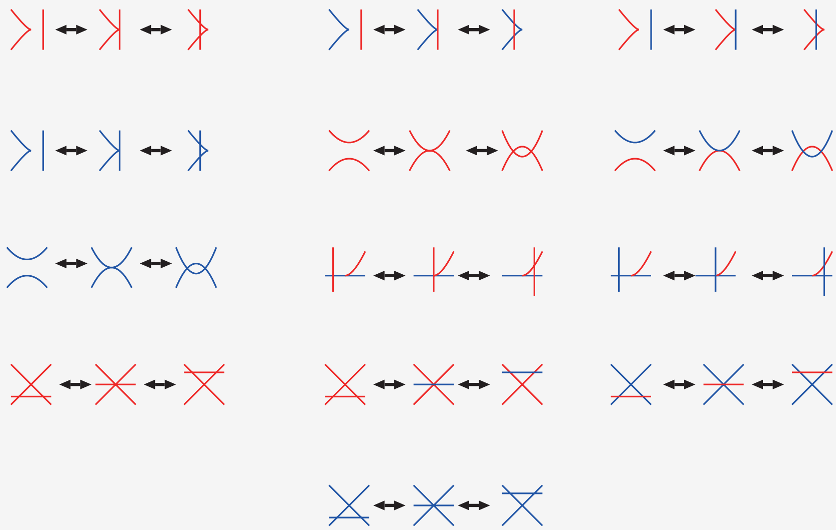

— Elimination of bdry singularities — 20/31

§ 3 Main-Theorem and Outline of a proof of Main-Theorem:

Let $H^n = \{(x_1, \dots, x_n) \in \mathbb{R}^n \mid x_n \geq 0\}$. Then, $\partial H^n = \{x_n = 0\}$.

Lemma 1.4(Characterization of B_2 Singularity)

$f\colon (H^2, 0) \to (\mathbb{R}^2, 0)$ a smooth map germ.

$(n = 2)$: f is B_2 singularity $\overset{\text{iff}}{\Leftrightarrow}$ $\begin{cases} f \text{ is **fold** if we ignore the bdry,} \\ f|_\partial \text{ is **immersion**,} \\ S(f) \pitchfork \partial \text{ at } 0. \end{cases}$

$(n = 3)$: f is B_2 singularity $\overset{\text{iff}}{\Leftrightarrow}$ $\begin{cases} f \text{ is **fold** if we ignore the bdry,} \\ f|_\partial \text{ is **fold**,} \\ S(f) \pitchfork \partial \text{ at } 0. \end{cases}$

! For a stable map $f\colon M \to P$ of an n-mfd $(n = 2, 3)$ with bdry into a surf. B_2 singularities are initial and terminal points of an arc component of $S(f)$. It implies that # of B_2 singularities of f is EVEN.

— Elimination of bdry singularities — 21/31

Lemma 1.5

M: a cpt n-mfd ($n = 2, 3$) with bdry, P: a surf. without bdry
$f\colon M \to P$: a stable map,
$S(f|_\partial) = S_1 \cup \cdots \cup S_\ell$, $\partial M = \partial_1 \cup \cdots \cup \partial_k$ the decomposition of $S(f|_\partial)$, ∂M into connected components resp. Then, we have the items below:
If $\dim M = 2$, then $^\#\{B_2\}$ is even on $\forall \partial_j$.
If $\dim M = 3$, then
(1) $^\#\{B_2\} + ^\#\{\text{bdry cusps}\}$ is even on $\forall S_i$, !!
(2) $^\#\{B_2\}$ and $\chi(\partial_j)$ have the same parity on $\forall \partial_j$. !!

! It yields that if $\dim M = 3$ and $\exists \partial_j \subset \partial M$ s.t. $\chi(\partial_j)$ is odd, then any stable map $f\colon M \to P$ has at least **ONE** B_2 point on $\partial_j \subset \partial N$.

! For the cases $\dim M \geq 4$, there are topological constraints of # of B_2 as well.

Main-Theorem A

M: a cpt n-mfd ($n = 2, 3$) with bdry, $\partial M = \partial_1 \cup \cdots \cup \partial_k$,
$f\colon M \to P$: a stable map.
($n = 2$): f is homotopic to a stable map $g\colon N \to P^2$ having **NO** B_2 points, namely, f is homotopic to a stable map $g\colon N \to P^2$ which is **SUBMERSION** on a sufficiently small nbd of ∂.
($n = 3$): Then, f is homotopic to a stable map $g\colon N \to P^2$ s.t.

$$\begin{cases} \text{if } \chi(\partial_j) \overset{(2)}{\equiv} 0, \text{ then } g \text{ has NO } B_2 \text{ points on } \partial_j, \\ \text{if } \chi(\partial_j) \overset{(2)}{\not\equiv} 0, \text{ then } g \text{ has ONE } B_2 \text{ point on } \partial_j. \end{cases}$$

In particular, if $\chi(\partial_j) \overset{(2)}{\equiv} 0$ for $^\forall \partial_j$, then f is homotopic to a stable map $g\colon M \to P^2$ which is **SUBMERSION** on a sufficiently small nbd of ∂M.

! The Theorem implies that g is obtained by applying local moves above finitely from f.

! We had obtained similar type theorem for the cases $\dim M \geq 4$.

To obtain a stable map $g\colon M \to P$ having NO B_2 pt.s, f is deformed by local moves given above following four steps below.

Step 1

$\dim M = 2$: Put $f_1 = f$.

$\dim M = 3$:

$$f \sim_{homotopic} f_1,$$

where f_1 is a stable map which have **NO** def-B_2 points.

! def-B_3-homotopy replace a def-B_2 point with a indef-B_2 point.

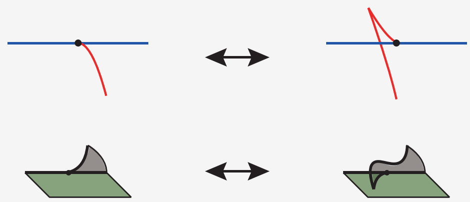

$S_1 \cup \cdots \cup S_\ell = S(f_1|_\partial)$, $p_{i_1}, \ldots, p_{i_k} \in S_i$: B_2 points which are ordered

Step 2

$$f_1 \sim_{homotopic} f_2,$$

where f_2 is a stable map s.t. there are

$$\begin{cases} \textbf{NO bdry cusps} \text{ among } p_{i_j} \text{ and } p_{i_{j+1}}, \text{ and} \\ \textbf{NO double point} \text{ among } f(p_{i_j}) \text{ and } f(p_{i_{j+1}}) \end{cases}$$

for each $j = 1, \ldots, k-1$.

! def/indef-C_3-homotopy replace an def/indef-B_2 point with a bdry cusp point.

Then, for each B_2 point p_i, $f_2(S(f_2) \cup S(f_2|_\partial))$ around p_i is locally one of the items below:

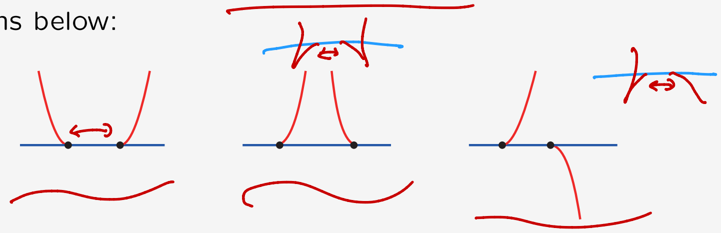

Step 3

$$f_2 \sim_{homotopic} f_3,$$

where f_3 is a stable map having **NO** B_2 points if $\dim M = 2$,

f_3 is a stable map s.t. $\#\{B_2\}$ points is **at most ONE** on $\forall S_i \subset S(f_3|_\partial)$ if $\dim M = 3$.

! Applying def/indef-B_3-homotopy and def/indef-B_2 beaks.

Step 4 **($\dim M = 3$)**

$$f_3 \sim_{homotopic} f_4,$$

where f_4 is a stable map s.t.

if $\chi(\partial_j) \overset{(2)}{\equiv} 0$, then $\#\{B_2\}$ points is **ZERO or TWO** on $^\forall S_i \subset S(f_4|_{\partial_j})$,

if $\chi(\partial_j) \overset{(2)}{\not\equiv} 0$, then $^{\exists_1} S_{i'} \subset S(f_4|_{\partial_j})$,

s.t. $\#\{B_2\}$ points is **ONE** on $S_{i'}$,

$\#\{B_2\}$ points is **ZERO or TWO** on $^\forall S_i \subset S(f_4|_{\partial_j}) \setminus S_{i'}$.

Then, by applying Steps 2 and 3 to f_4, we obtain the desired stable map $g\colon M \to P^2$.

To apply STEP 4, there are two cases for f_3:

Case (1) $\gamma \subset S(f)$: an arc whose bdry is a pair of B_2 points $p_1, p_2 \in \partial_j$ s.t. $p_1 \in S_{j_1}$ and $p_2 \in S_{j_2}$ ($S_{j_1}, S_{j_2} \subset S(f|_{\partial_j})$).

Assume that for p_1 and p_2, $^{\exists}$bdry cusps in the sufficiently small nbd of p_1, p_2 resp. Then, by using C_3-homotopy if necessary, we obtain the following lemma.

Lemma 3.1

Let η be an embedded curve transversal to $S(f_3|_\partial)$ with $\eta(0) = p_\lambda$, $\eta(1) = p_\mu$ s.t. there are NO bdry cusps f_3 on $\eta((0,1))$. Then, $\exists$ a homotopy s.t. the homotopy does NOT change f_3 on $N \setminus N(\eta)$ and it change f_3 to a stable map which has no cusps on $N(\eta)$.

Case (2): $\gamma_\lambda \subset S(f)$: arc whose bdry are $p_{\lambda_1} \in \partial_{j_1}$ and $p_{\lambda_2} \in \partial_{j_2}$, $\gamma_\mu \subset S(f)$: arc whose bdry are $p_{\mu_1} \in \partial_{j_1}$ and $p_{\mu_3} \in \partial_{j_3}$.

Assume that for p_{λ_1} and $p_{\lambda_2}, p_{\mu_1}, p_{\mu_3}$, there are bdry cusps in the sufficiently small nbhd of p_{λ_1} and $p_{\lambda_2}, p_{\mu_1}, p_{\mu_3}$ resps. Then, by using C_3-homotopy and Sw.-homotopy if necessary, we obtain the following Lemma.

Lemma 3.2

Let η be an embedded curve transversal to $S(f_3|_\partial)$ with $\eta(0) = p_{\lambda_1}$, $\eta(1) = p_{\mu_1}$ s.t. there are NO bdry cusps on $\eta((0,1))$. Then, $\exists$ a homotopy s.t. the homotopy does NOT change f_3 on $N \setminus N(\eta)$ and it change f_3 to a stable map which has no cusps on $N(\eta)$.

□

Main-Theorem B

Let M be a **3-mfd** with bdry s.t. $\chi(\partial_j) \overset{(2)}{\equiv} 0$ for ${}^{\forall}\partial_j \subset \partial M$,
$f : M \to \mathbb{R}^2$ a stable map.
Then, f is homotopic to a stable map which have
NO B_2 points and **NO bdry cusp points**.

Thank you for your attention!

Simplifying Indefinite Fibrations on 4–manifolds

Osamu Saeki (Kyushu Univ.)

Joint work with **İnanç BAYKUR** (Univ. of Massachusetts)

Fiber Topology Meets Applications
at Kyushu University

January 8, 2021

§1. Broken Lefschetz Fibrations

Lefschetz Fibration

In this talk, manifolds and maps are differentiable of **class** C^∞.

Definition 1.1
M^4, Σ^2: closed (= compact w/o boundary) **oriented** manifolds

A **singularity** of a smooth map $M^4 \to \Sigma^2$ that has the normal form

$$\boxed{(z, w) \mapsto zw}$$

w.r.t. "C^∞ complex coordinates" compatible with the orientations, is called a **Lefschetz** singularity.

A smooth map $M^4 \to \Sigma^2$ is a **Lefschetz fibration** (**LF**) if it has only Lefschetz singularities.

Lefschetz Pencil

Lefschetz pencil (**LP**) is a **LF** $M^4 \setminus B \to S^2$ for a finite set $B \neq \emptyset$, where it has complex local model

$$(z_1, z_2) \mapsto z_1/z_2 \in \mathbf{C} \cup \{\infty\} = S^2.$$

(**Blowing-up** the points in B, we get a **LF** $M^4 \sharp (\sharp^{|B|} \overline{\mathbf{C}P^2}) \to S^2$.
Conversely, **blowing-down** (-1)-sections for a LF, we get a **LP**.)

Donaldson, Gompf, Late 90's
$\exists$**Lefschetz pencil** $\Longleftrightarrow$ $\exists$**symplectic structure**

Symplectic structure: $\omega \in \Omega^2(M^4)$, $d\omega = 0$, non-degenerate $(\omega^2 > 0)$

⚠Symplectic structures are "**HARD**" to find.

Broken Lefschetz Fibration

Definition 1.2 A **singularity** that has the (real) normal form

$$\boxed{(t, x_1, x_2, x_3) \mapsto (t, x_1^2 + x_2^2 - x_3^2)}$$

is called an **indefinite fold** singularity.

Definition 1.3 (Auroux-Donaldson-Katzarkov, 2005)
$f : M^4 \to \Sigma^2$ is a **broken Lefschetz fibration** (**BLF**) if it has at most Lefschetz and indefinite fold singularities.
Broken Lefschetz pencil (**BLP**) is similarly defined.

Z_f: set of **indefinite fold sing.** $\leftarrow$ closed 1-**dim. submanifold** of M^4

Near-symplectic Structures

Auroux-Donaldson-Katzarkov, 2005
$\exists$**broken Lefschetz pencil** $\Longleftrightarrow$ $\exists$**near-symplectic structure**

Near-symplectic structure: $\omega \in \Omega^2(M^4)$, $d\omega = 0$, $\omega^2 \geq 0$,
ω vanishes along a 1-**dim. submanifold** Z_ω "transversely".

Example 1.4 $\Omega = dt \wedge dQ + *(dt \wedge dQ)$ on $\mathbf{R}^4$ with coordinates (t, x_1, x_2, x_3) is such an example with $Z_\Omega = t$-axis.
Here, $Q(x_1, x_2, x_3) = x_1^2 + x_2^2 - x_3^2$ and $*$ is the Hodge star operator.

Near-symplectic structures are "**EASY**" to find.

In this talk, I will explore **BLF** and **BLP** from **singularity theoretical viewpoints**.

§2. Indefinite Fibrations

Indefinite Fibration

A **singularity** of $M^4 \to \Sigma^2$ is a **fold** if it is locally given by
$(t, x_1, x_2, x_3) \mapsto (t, \pm x_1^2 \pm x_2^2 \pm x_3^2)$.
A **singularity** is a **cusp** if it is locally given by
$(t, x_1, x_2, x_3) \mapsto (t, x_1^3 + tx_1 \pm x_2^2 \pm x_3^2)$.

Whitney, Thom, ~1950's
Any smooth map can be approximated by a map with only **fold and cusp singularities**. (Such $f : M^4 \to \Sigma^2$ is called a **generic map**.)

f is an **indefinite generic map** if its folds and cusps are all **indefinite**.

$f : M^4 \to \Sigma^2$ is an **indefinite fibration** (**IF**) if it has at most indefinite folds, indefinite cusps, and **Lefschetz** singularities.

Various Classes of Maps

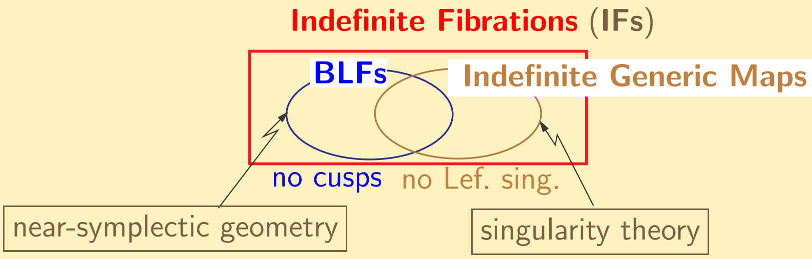

Main Objective

§1. Broken Lefschetz Fibrations §2. Indefinite Fibrations §3. Moves §4. Constructions §5. Trisections

Main objective of this talk is to provide **explicit "algorithms"** to **simplify** the topology of IFs to get nice fold images as follows:

BLF with **directed embedded** fold image.

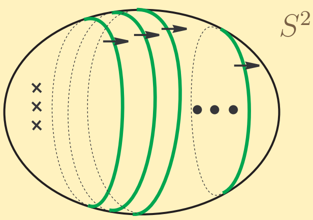

New Proof of ADK Theorem

As a result, we can give a **purely topological proof** to the following.

Theorem 2.1 (Auroux-Donaldson-Katzarkov, 2005)
M^4: *closed oriented* 4*-manifold.*
(1) $Z \neq \emptyset$: *closed oriented* 1*-dim. submanifold of* M^4
s.t. $[Z] = 0$ *in* $H_1(M^4; \mathbf{Z})$
$\Longrightarrow$ $\exists$**fiber-connected BLF** $f : M^4 \to S^2$ *with* **simplified fold image** *s.t.* $Z_f = Z$.

(2) $\exists$**near-symplectic form** ω *with* $Z_\omega \neq \emptyset$
$\Longrightarrow$ $\exists$**fiber-connected BLP** g *on* M^4 *with* **simplified fold image** *s.t.* $Z_g = Z_\omega$.

In particular, **every closed oriented 4-manifold admits a BLF**.
Our "algorithms" are based on sing. theory and give **explicit** constructions of **BLF** and **BLP** that are **simplified**.

§1. Broken Lefschetz Fibrations §2. Indefinite Fibrations §3. Moves §4. Constructions §5. Trisections

§3. Moves

Fibers of an IF

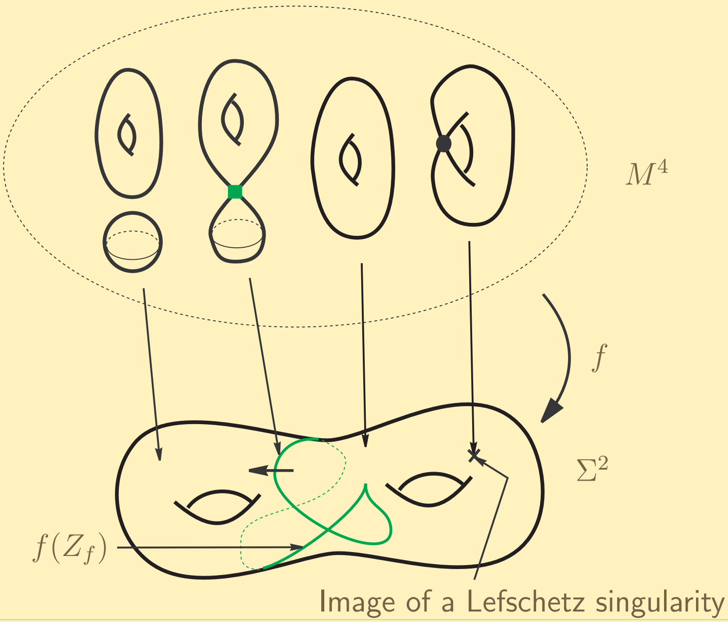

Normal Orientation

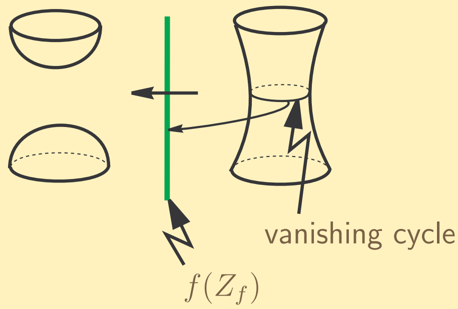

Fold image

The image of indefinite folds is **normally oriented**.

Base Diagram

For an IF $f : M^4 \to \Sigma^2$, **base diagram** is the pair $(\Sigma^2, f(Z_f \cup L_f))$.

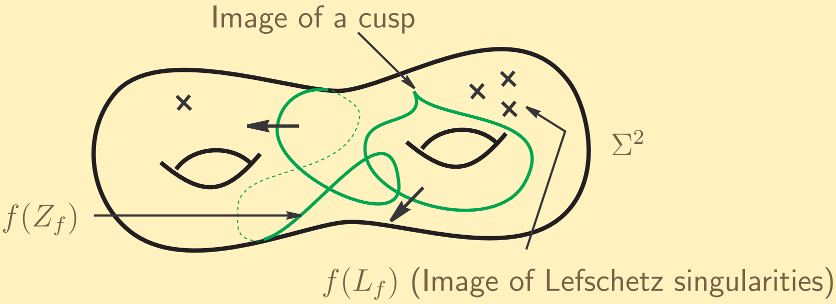

Moves for Indefinite Fibrations

Definition 3.1 A **move** for an IF $f : M^4 \to \Sigma^2$ is a smooth 1-parameter family $f_t : M^4 \to \Sigma^2$, $t \in [0, 1]$, of "mostly" IFs, with $f_0 = f$, which modifies the base diagram only in a nbhd of a point in Σ^2.
(Except for finitely many t's, f_t is an IF.)

Definition 3.2 A move is **always-realizable** if, given a local configuration of a base diagram, we can **always** find a 1-parameter family as above that realizes the relevant base diagram change.

Moves I

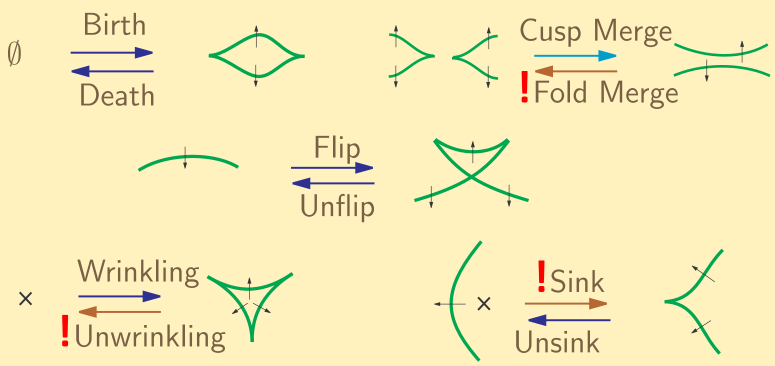

Blue arrows are **always-realizable**, while **brown arrows are not**.
Cusp Merge is "always-realizable" as long as the fibers are connected.

Moves II

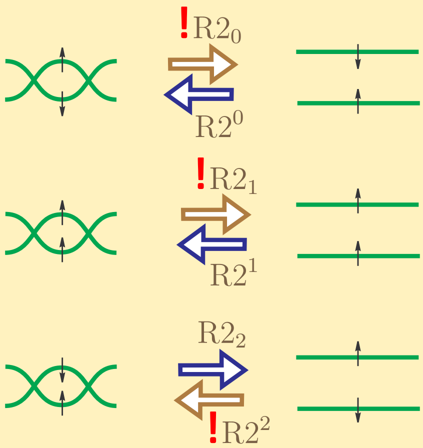

Reidemeister II type moves

Moves III

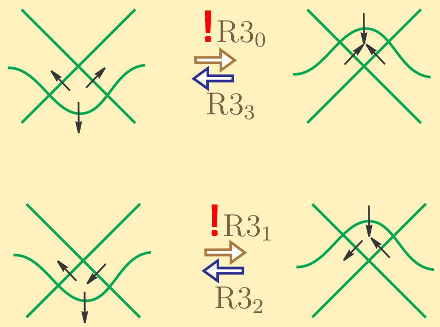

Reidemeister III type moves

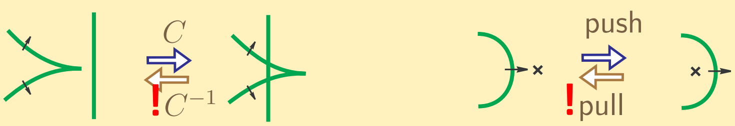

Cusp-fold crossing & push/pull moves □

§4. Constructions

Directed Fold Image

Lemma 4.1 *There exists an explicit* **"algorithm"** *consisting of* **always-realizable moves**, *which makes any given IF* **directed**.

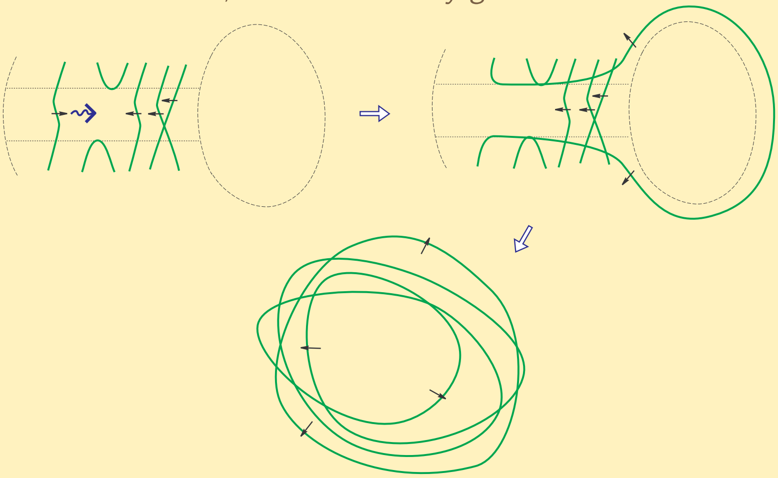

□

Directed Embedded Fold Image

Lemma 4.2 *There exists an explicit* **"algorithm"** *consisting of* **always-realizable moves**, *which turns any given* **directed** *IF into a* **directed** *one with* **embedded fold image**.

Using certain always-realizable moves, we can arrange so that each "component" winds exactly once.

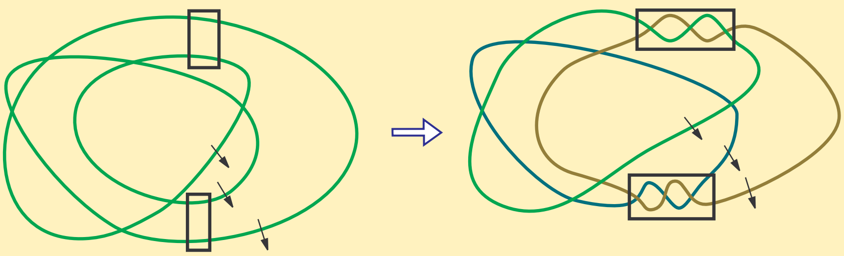

Then, we can reduce crossings using Reidemeister type moves. □

Simplified BLF

Then, we get the following.

Theorem 4.3 M^4: *closed ori. 4-manifold,*
$Z \neq \emptyset$: $[Z] = 0$ *in* $H_1(M; \mathbf{Z})$.
$\Longrightarrow$ $\exists$**fiber-connected BLF** $f: M^4 \to S^2$ *with* **directed, embedded fold image** *s.t.* $Z_f = Z$.

Proof starts with a generic map $M^4 \to S^2$ which may not be indefinite.

Theorem 4.4 (S., 2006)
$\forall f : M^4 \to S^2$ *is homotopic to an indefinite generic map* **without definite folds**.

In other words, we can eliminate **definite folds** by homotopy.

We can now apply **our "algorithms"**. □

§5. Trisections

Trisection

Gay–Kirby (2013) showed that **every** connected closed orientable 4-**manifold** M^4 admits a generic map into $\mathbf{R}^2$ whose image is as follows.

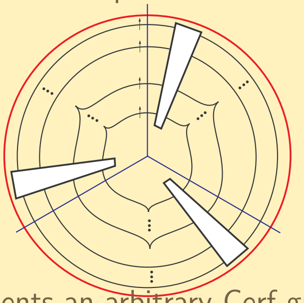

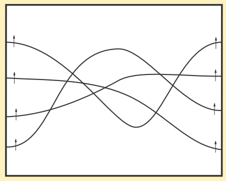

Each box represents an arbitrary Cerf graphic as in the right.
Then, the three half lines divide the image into three parts and their inverse images are all diffeomorphic to $\natural(S^1 \times D^3)$.

Every 4-manifold admits such a **trisection**.

Simplified Trisection

Our explicit "algorithm" for simplifying an IF leads to the following.

Theorem 5.1 *Every M^4 admits a* **simplified trisection** (**ST**), *i.e. a trisection with trivial Cerf graphics.*

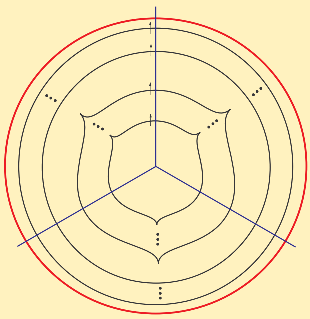

Image of a simplified trisection

Genera of BLF and ST

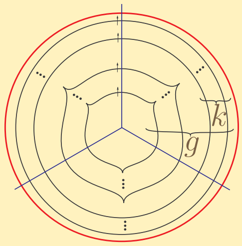

Simplified (g,k)-trisection $=$ (g,k)-ST

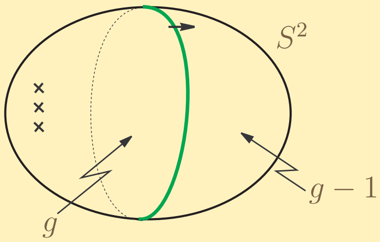

Simplified BLF with genus g $=$ g-SBLF

Bridging SBLFs and STs

Our explicit constructions lead to the following.

Theorem 5.2 *Suppose M^4 admits a g-**SBLF**, with $k \geq 0$ Lefschetz sing., and $\ell \in \{0,1\}$ components of Z_f.*
$\Longrightarrow \exists$ (g',k')-**ST** *of M^4 with*
$g' = 2g + k - \ell + 2$ *and* $k' = 2g - \ell$.

*Conversely, suppose M^4 admits a (g',k')-**ST**.*
$\Longrightarrow \exists$ g-**SBLF** *with k Lefschetz sing. and one Z_f component, where*
$g = g' + 3$ *and* $k = 5g' - 3k' + 8$.

In fact, given an explicit **SBLF** (or **ST**), we can EXPLICITLY construct an associated **ST** (resp. **SBLF**).

Thank you for your attention !

References:

- R.I. Baykur and O. Saeki, Simplified broken Lefschetz fibrations and trisections of 4-manifolds, Proc. Natl. Acad. Sci. USA 115 (2018), 10894-10900.
- R.I. Baykur and O. Saeki, Simplifying indefinite fibrations on 4-manifolds, to appear in Trans. Amer. Math. Soc.

An Efficient Triangulation for Extruded Spatiotemporal Prism Meshes

Akito Fujii
Kenji Ono
Daisuke Sakurai

1

Triangulation of spatiotemporal meshes

- Contour tree requires spatial triangulation
- Thanks to in-situ analysis, very fine temporal resolution!
- We want to triangulate spatiotemporal meshes without breaking pre-defined spatial triangulation

2

Constructing spatiotemporal mesh is difficult

- Delaunay-based triangulation : difficult to implement
  - CGAL does not offer implementation even for 3D
  - Processing for numerical errors
    - special module such as Arbitrary-precision arythmetic is necessary
- Slow
- Parallelism is difficult
  - A lot of communication at the boundary of data

3

Our proposed spatiotemporal triangulation!

- Implicit :
  - On-the-fly from the information in the node
  - Ex. crystalline triangulation
- Features :
  - Arbitrary dimension
  - Arbitrary spatial triangulation
  - Extrude to time direction
  - Fast
  - Parallelism
- Assume temporally static meshes

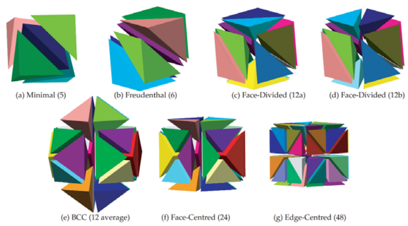

[Carr et.al. 2006, IEEETVCG]

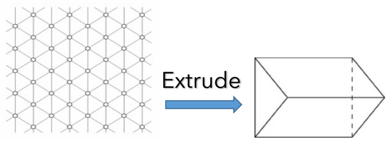

4

Conclusion

- We propose triangulation algorithm for extruded prism meshes
  - This algorithm can apply meshes in arbitrary dimensions
- Low cost
  - Cost does not depend on the number of vertices
  - We do not have to store triangulation of meshes
  - Look up table for the triangulation only depends on the number of dimension
  - Easy to implement

6

「マス・フォア・インダストリ研究」シリーズ刊行にあたり

本シリーズは，平成 23 年 4 月に設立された九州大学マス・フォア・インダストリ研究所(IMI)が，平成 25 年 4 月に共同利用・共同研究拠点「産業数学の先進的・基礎的共同研究拠点」として，文部科学大臣より認定を受けたことにともない刊行するものである．本シリーズでは，主として，マス・フォア・インダストリに関する研究集会の会議録，共同研究の成果報告等を出版する．各巻はマス・フォア・インダストリの最新の研究成果に加え，その新たな視点からのサーベイ及びレビューなども収録し，マス・フォア・インダストリの展開に資するものとする．

平成 30 年 10 月
マス・フォア・インダストリ研究所
所長 佐伯　修

Fiber Topology Meets Applications

マス・フォア・インダストリ研究 No.21, IMI，九州大学
ISSN 2188-286X
発行日　2021 年 3 月 10 日
編　集　Daisuke Sakurai, Shigeo Takahashi, Naoki Hamada, Osamu Saeki, Hamish Carr
Takahiro Yamamoto
発　行　九州大学マス・フォア・インダストリ研究所
〒819-0395 福岡市西区元岡 744
九州大学数理・IMI 事務室
TEL 092-802-4402　FAX 092-802-4405
URL https://www.imi.kyushu-u.ac.jp/
印　刷　城島印刷株式会社
〒810-0012 福岡市中央区白金 2 丁目 9 番 6 号
TEL 092-531-7102　FAX 092-524-4411

シリーズ既刊

Issue	Author ／ Editor	Title	Published
マス・フォア・インダストリ研究　No.1	穴田　啓晃 安田　貴徳 Xavier Dahan 櫻井　幸一	Functional Encryption as a Social Infrastructure and Its Realization by Elliptic Curves and Lattices	26 February 2015
マス・フォア・インダストリ研究　No.2	滝口　孝志 藤原　宏志	Collaboration Between Theory and Practice in Inverse Problems	12 March 2015
マス・フォア・インダストリ研究　No.3	筧　三郎	非線形数理モデルの諸相：連続，離散，超離散，その先 (Various aspects of nonlinear mathematical models : continuous, discrete, ultra-discrete, and beyond)	24 March 2015
マス・フォア・インダストリ研究 No.4	穴田　啓晃 安田　貴徳 櫻井　幸一 寺西　勇	Next-generation Cryptography for Privacy Protection and Decentralized Control and Mathematical Structures to Support Techniques	29 January 2016
マス・フォア・インダストリ研究 No.5	藤原　宏志 滝口　孝志	Mathematical Backgrounds and Future Progress of Practical Inverse Problems	1 March 2016
マス・フォア・インダストリ研究 No.6	松谷　茂樹 佐伯　修 中川　淳一 上坂　正晃 濵田　裕康	結晶のらせん転位の数理	10 January 2017
マス・フォア・インダストリ研究 No.7	滝口　孝志 藤原　宏志	Collaboration among mathematics, engineering and industry on various problems in infrastructure and environment	1 March 2017
マス・フォア・インダストリ研究 No.8	藤原　宏志 滝口　孝志	Practical inverse problems based on interdisciplinary and industry-academia collaboration	20 February 2018
マス・フォア・インダストリ研究 No.9	阿部　拓郎 高島　克幸 縫田　光司 安田　雅哉	代数的手法による数理暗号解析 Workshop on analysis of mathematical cryptography via algebraic methods	1 March 2018
マス・フォア・インダストリ研究 No.10	阿部　拓郎 落合　啓之 高島　克幸 縫田　光司 安田　雅哉	量子情報社会に向けた数理的アプローチ Mathematical approach for quantum information society	26 December 2018

Issue	Author ／ Editor	Title	Published
マス・フォア・インダストリ研究 No.11	松谷　茂樹 佐伯　修 中川　淳一 濵田　裕康 上坂　正晃	結晶転位の先進数理解析 Advanced Mathematical Investigation for Dislocations	7 January 2019
マス・フォア・インダストリ研究 No.12	滝口　孝志	Non-destructive inspection for concrete structures and related topics	13 February 2019
マス・フォア・インダストリ研究 No.13	宇波　耕一 長野　智絵 吉岡　秀和 田上　大助 白井　朋之	数理農学における時系列データのモデル化と解析 Modeling and Analysis of Time Series Data in Math-Agro Sciences	28 February 2019
マス・フォア・インダストリ研究 No.14	佐久間　弘文 大津　元一 小嶋　泉 福本　康秀 山本　昌宏 納谷　昌之	ドレスト光子に関する基礎的数理研究	18 March 2019
マス・フォア・インダストリ研究 No.15	松谷　茂樹 佐伯　修 中川　淳一 濵田　裕康 富安　亮子	結晶の界面，転位，構造の先進数理解析	2 December 2019
マス・フォア・インダストリ研究 No.16	Takuro Abe Yasuhiko Ikematsu Koji Nuida Yutaka Shikano Katsuyuki Takashima Masaya Yasuda	Quantum computation, post-quantum cryptography and quantum codes	17 January 2020
マス・フォア・インダストリ研究 No.17	河村　彰星 津曲　紀宏 西澤　弘毅 溝口　佳寛	代数・論理・幾何と情報科学―理論から実世界への展開	10 February 2020
マス・フォア・インダストリ研究 No.18	Takashi Takiguchi	New technologies for non-destructive and non-invasive inspections and their applications	21 February 2020
マス・フォア・インダストリ研究 No.19	Hirofumi Sakuma Motoichi Ohtsu Masayuki Naya Izumi Ojima Yasuhide Fukumoto	Basic mathematical studies on dressed photon phenomena	19 March 2020

マス・フォア・インダストリ
研究 No.20

松谷　茂樹
井上　和俊
加葉田雄太朗
佐伯　　修
垂水　竜一
内藤　久資
中川　淳一
濵田　裕康

材料科学における幾何と代数 I

24 November 2020

Institute of Mathematics for Industry
Kyushu University

九州大学マス・フォア・インダストリ研究所
〒819-0395 福岡市西区元岡744
https://www.imi.kyushu-u.ac.jp